REPORT DOCUMENTATION PAGE

Form Approved
OMB No. 0704-0188

1. REPORT DATE *(DD-MM-YYYY)*	2. REPORT TYPE	3. DATES COVERED *(From - To)*
12/18/2014	Final Performance/Technical Report	7/1/2011 - 9/30/2014

4. TITLE AND SUBTITLE
Understanding Solidification Based Grain Refinement in Steels

5a. CONTRACT NUMBER

5b. GRANT NUMBER
N00014-11-1-0492

5c. PROGRAM ELEMENT NUMBER

6. AUTHOR(S)
Tuttle, Robert

5d. PROJECT NUMBER
14PR03640-03

5e. TASK NUMBER

5f. WORK UNIT NUMBER

7. PERFORMING ORGANIZATION NAME(S) AND ADDRESS(ES)
Saginaw Valley State University
7400 Bay Road
University Center, MI 48710

8. PERFORMING ORGANIZATION REPORT NUMBER

9. SPONSORING/MONITORING AGENCY NAME(S) AND ADDRESS(ES)
ONR Reg. Office Chicago - N62880
230 South Dearborn, Room 380
Chicago, IL 60604-1595

10. SPONSOR/MONITOR'S ACRONYM(S)
ONR

11. SPONSOR/MONITOR'S REPORT NUMBER(S)

12. DISTRIBUTION/AVAILABILITY STATEMENT
Approved for Public Release; distribution is Unlimited.

13. SUPPLEMENTARY NOTES

14. ABSTRACT
The overall goals for this project are to elucidate the grain refinement mechanism in cast steels, develop a master grain refining alloy, and determine how heat treatment affects grain refined structures.
Specific objectives: 1) Determine the cause of intermittent grain refinement in 1010 and 1030 alloys with rare earth additions. 2) Create a master alloy based on rare earth oxides. 3) Extend steel solidification knowledge by understanding how nucleation events occur. 4) Examine how industrial heat treatments affect the structure and properties of grain refined steels. 5) Determine if heat treatments can be modified to improve properties for grain refined steels.

15. SUBJECT TERMS
steel, casting, foundry, grain refinement, mechanical properties, solidification, heterogeneous nucleation

16. SECURITY CLASSIFICATION OF:			17. LIMITATION OF ABSTRACT	18. NUMBER OF PAGES	19a. NAME OF RESPONSIBLE PERSON
a. REPORT	b. ABSTRACT	c. THIS PAGE			Robert Tuttle
u	u	u	uu	37	19b. TELEPHONE NUMBER *(Include area code)* 989-964-4676

Standard Form 298 (Rev. 8/98)
Prescribed by ANSI Std. Z39.18

20141219283

Instructions: You may use this MS Word file as a guideline to submit the Technical Section (# 4) of the ONR End of Year Report. In this Technical Section, you are encouraged to include any images, tables, graphs, and equations that you feel may strengthen the technical quality of your report. The Technical Section must include the ***Objectives, Approach,* and *Progress*** completed since your last report. If this is a new effort or continuing work under an extension, the report should cover work completed during this FY. Please complete the ***Award Information*** section below so that technical information can be related to a specific award.

Please save the file using the award number as the file name (e.g. N0001496C0387.doc).

If you have any questions with this form or with the web site, please contact the help desk at Code_33_EOY_Report@ONR.NAVY.MIL

Award Information

Award Number	N000141110492
Title of Research	Understanding Solidification Based Grain Refinement in Steels
Principal Investigator	Dr. Robert Tuttle
Organization	Saginaw Valley State University

Technical Section

Technical Objectives

The overall goals for this project are to elucidate the grain refinement mechanism in cast steels, develop a master grain refining alloy, and determine how heat treatment affects grain refined structures.

Specific objectives:

1) Determine the cause of intermittent grain refinement in 1010 and 1030 alloys with rare earth additions.
2) Create a master alloy based on rare earth oxides.
3) Extend steel solidification knowledge by understanding how nucleation events occur.
4) Examine how industrial heat treatments affect the structure and properties of grain refined steels.
5) Determine if heat treatments can be modified to improve properties for grain refined steels.

Technical Approach

Grain size reduction is regularly practiced in steel mills. Controlled hot rolling and grain size reduction via inhibiting austenite grain growth have led to significant strength improvements in the strength of steels.[1-20] Reducing the grain size improves strength through Hall-Petch strengthening. This strengthening results from the shorter distance a dislocation can travel through a metal crystal before being blocked by a grain boundary. Since the dislocation is impeded sooner, the material cannot deform the same magnitude thereby increasing strength.

Steel foundries cannot use thermomechanical methods for decreasing grain size. Steel castings are produced by making a mold using a pattern in the shape of the part. The pattern is removed, and the resulting mold has a cavity for the part. Liquid steel poured into the mold freezes into the shape of the desired part. Minor machining or a heat treatment for properties is all that is usually required to create a finished component. Since the casting is near final shape, any mechanical deformation to develop properties results in an unsalable casting. Mechanical deformation would also result in increased manufacturing cost which negates the advantages of the metalcasting process.

Therefore, reducing grain size requires a different approach. Grain refinement through the manipulation of heterogeneous nucleation presents an opportunity for reducing grain size. The concept is to introduce a large number of heterogeneous nuclei to increase the number of grains that grow from the liquid. These grains impinge on each other earlier during solidification which limits their size. Effective heterogeneous nuclei must meet four criteria: 1) be solid at the solidification temperature of the melt; 2) be thermodynamically stable in the melt; 3) be wetted by the liquid metal; and 4) have a similar crystallographic structure to the host metal. Using reference data and thermodynamic calculations, criteria 1 and 2 are readily verifiable. Wetting data for liquid metals is frequently unavailable to make a decision about the suitability for a particular candidate phase. Criteria 4 is evaluated by examining the difference in lattice parameters between the nuclei candidate and metal. The difference in lattice parameters has been referred to as the lattice disregistry.[21] The Turnbull-Vonnegut equation calculates this lattice disregistry.[21] Equation 1 is for cubic crystals:

$$\delta = \frac{\delta_1 + \delta_2 + \delta_3}{3} * 100 \qquad (1)$$

where δ_1, δ_2, and δ_3 = the disregistries along the three lowest-index directions within a 90° quadrant of the planes in the nucleated solid and substrate. A more general form of this equation is:

$$\delta_{(hkl)_n}^{(hkl)_s} = \sum_{i=1}^{3} \frac{\dfrac{\left|(d_{[uvw]_s^i} \cos\theta) - d_{[uvw]_n^i}\right|}{d_{[uvw]_n^i}}}{3} * 100 \qquad (2)$$

where $(hkl)_s$ = a low-index plane of the substrate, $[uvw]_s$ = a low-index direction in $(hkl)_s$, $(hkl)_n$ = a low-index plane in the nucleated solid, $[uvw]_n$ = a low-index direction in $(hkl)_n$, $d_{[uvw]n}$ = the interatomic spacing along $[uvw]_n$, $d_{[uvw]s}$ = the interatomic spacing along $[uvw]_s$, and
θ = the angle between the $[uvw]_s$ and $[uvw]_n$.[21]

Work on the grain refinement of aluminum and magnesium alloys has found that strongly segregating elements are necessary to produce the finest structure possible with a particular heterogeneous nuclei.[22-32] The earliest observations of this phenomena were related to determining why wrought aluminum and cast aluminum alloys responded differently to the same heterogeneous nuclei additions.[22] Currently, it is understood that strongly segregating alloying elements preferentially remain in the liquid during solidification. The resulting enrichment of the liquid locally reduces the liquidus temperature of the alloy and increases constitutional undercooling.[22, 25, 26] The increase in constitutional undercooling provides a larger driving force for nucleation and decreases the dendrite growth rate.[22, 25, 26, 30] Growth restriction can also occur due to other solidification factors.[22] The growth restriction factor (GRF) can be used to predict reductions in growth rate.[22]

$$GRF = mc_o(k-1) \quad (4)$$

where m = the gradient of the liquidus, c_o = the concentration of the solute in the alloy, and k = the partition coefficient. Partition coefficients are determined by the following equation:

$$k = \frac{c_s}{c_l} \quad (5)$$

where c_s = the composition of the solid and c_l = the composition of the liquid at the temperature of the solidification front.

Developing grain refinement techniques for steel that utilize a solidification approach is the only method suitable for steel castings. The method also has the advantage that it could also be adopted by steel mills. Creating a suitable solidification based grain refinement method will require creating an addition which contains both heterogeneous nuclei and a strongly segregating element that encourages nucleation in the melt.

Rare earth additions proved to be a promising grain refining avenue in the previous project and will be the focus of this project. It is still not apparent the exact mechanism producing refinement with rare earth additions. Understanding the mechanism is key for developing a reliable industrial technology. Elucidating the mechanism will require additional experimental castings to be poured and a series of static phase equilibrium experiments. As most steel castings undergo some type of heat treatment, it is also necessary to understand how heat treatment and grain refinement interact. A series of heat treatment experiments are being proposed in this project to develop knowledge about that interaction.

Understanding the inconsistent results obtained in rare earth grain refined steels requires a more thorough investigation of the fundamental mechanism involved. Rare earth (RE) oxides of the form RE_2O_3 and REO_2 have been reported as effective nuclei.[33-38] However, refinement of the microstructure in steel has been reported to occur by some authors and not by others, similar to experiments in the previous project by the PI. To address this knowledge deficiency, the PI will conduct additional experiments on the addition of rare earth containing steels.

The first series of experiments will consist of increasing the rare earth additions. Many of the heats from the previous project had rare earth levels below 0.09%, significantly below the target total rare earth levels. It is possible that successful refinement must be above a certain value which was not achieved in those experiments. Transmission electron microscopy (TEM) will also be conducted to determine how small rare earth oxides are distributed in the steel. Since no examination of nano sized particles in the matrix was conducted in the previous study, it is not possible to determine if there was a difference in those particles which led to the observed structural and strength differences between steels with the same rare earth content.

Furthermore, the PI plans on applying a new electron microscope to samples from this project. The machine, made by ASPEX, consists of a small scanning electron microscope (SEM) with a back scatter detector and an energy dispersive spectrometer (EDS). Several samples can be loaded simultaneously. The unit employs the high degree of Z contrast between the steel matrix and inclusions to determine when an inclusion is present. When an inclusion is detected, the unit acquires an EDS spectrum and continues to search for more inclusions. The machine is automated so over 1,000 inclusions can be examined from a single sample. The resulting inclusion data can be plotted in various ways. One of the most common

methods is to plot the composition of each inclusion on a ternary phase diagram to visualize the chemical and size distribution (See Figure 13). The PI recently became aware of this tool and has access to a unit.

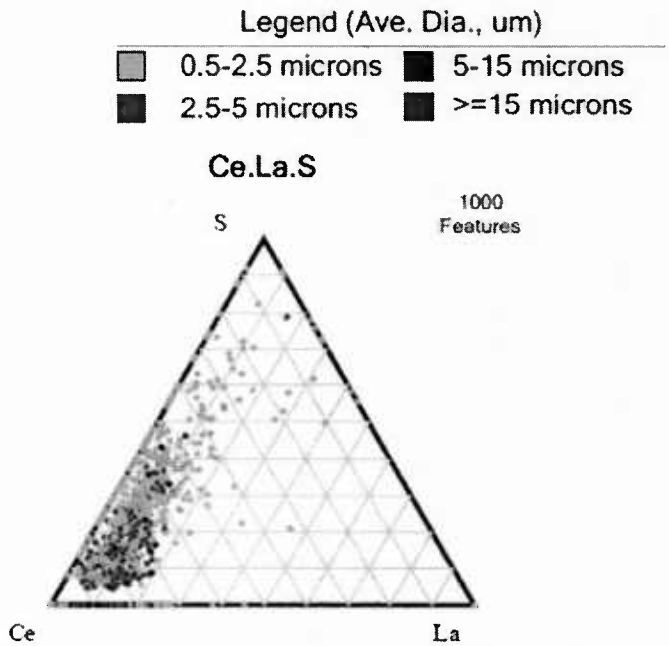

Figure 1 Inclusion size and chemistry ternary plot from ASPEX system.

The author found some evidence of reactions occurring with some rare earth oxide or sulfide inclusions and iron or aluminum oxides. If this reaction causes the loss in grain refinement, it could explain the inconsistent results obtained in the previous project. One cause of these iron or aluminum oxides is reoxidation during tapping. The rare earth additions were added during tapping which may have allowed them to incorporate these oxides. To examine the role iron or aluminum oxides may play in "poisoning" grain refinement, the PI plans on conducting a series of experiments under an argon atmosphere. Small 0.25 inch diameter holes will be drilled into refractory samples. Steel rods and small amounts of rare earth metal or RE oxides would be added to the hole in the refractory. The refractory-steel sample could then be heated in a small furnace to 1600°C under argon. After a set period at temperature, the samples would cool to room temperature. The argon would prevent reoxidation of the steel while it melts and thereby protect the RE oxides that form. The resulting inclusions and steel would be examined for grain refinement and inclusion chemistry. In addition to varying levels of rare earth content and RE oxides, different refractories could be tested to determine if reactions with the refractory are causing changes. There is little information in the literature about rare earth oxide inclusions reacting with refractories. Golikov conducted experiments on rare earth oxides and manganese oxides when heated in air.[46] There has also been work on how rare earth oxides affect alumina and silica cements and aggregates in refractories.[47,48] However, no work appears to have been done on what happens to rare earth oxide inclusions based on the type of refractory used.

The next thrust area for this project will develop an understanding of how refinement affects the heat treatment of fine grained steels. This area really has two facets. One will be determining how the properties of grain refined steels change with standard heat treatments. The second facet that will be investigated is how the heat treatment cycle can be modified to produce superior mechanical properties to current foundry practice.

For the first series of heat treatment experiments, a set of 1030 test plates will be poured with rare earth refinement practice. These plates will be normalized using standard practice. Hardness, tensile testing, and metallographic examination will be conducted after the heat treatment. The goal of these experiments is to simply observe the resulting structure-property relationship. Data from these experiments will provide a guideline to the next set of experiments.

A second series of heat treatment experiments will be done to determine how heat treatment practice can be changed. Finer grained metals have reduced microsegregation.[27-29] The reduction in microsegregation should reduce the time required for those elements to diffuse through the microstructure. A reduction in the time required for solid state reactions such as the nucleation and growth of new austenite grains during austenization is the expected result. A set of cast 1030 test plates will be poured using grain refinement practice. The plates will be austenitize for different lengths of time to determine how soon austenization can be stopped. Determining when the microstructure has been fully transformed to austenite will be done by microstructural examination.

Using observations from the previously mentioned experiments, the PI wants to create a master alloy type addition to routinely produce grain refinement. The goal of this is to demonstrate that a sufficient understanding of heterogeneous nucleation and grain refinement of steels has been developed by creating a functional master alloy. Creating a master alloy will require one of two experimental routes. The first is to simply melt a heat of steel or other suitable base metal and conduct a reaction within a furnace. Round rod samples could be extracted using a vacuum sampling system with a quartz tube. These rods could be then added to a heat of 1010 or 1030 during tapping to introduce the desired nuclei. Based on the thermodynamic stability of rare earth species in steel melts and their crystallographic structure, the most likely desired phases would be either an oxide or sulfide.[33-38] Another approach would be to react a sample of misch metal or rare earth silicide at elevated temperatures to form the desired oxide or sulfide species. In either approach, the key will be to form the nucleating compound identified in the previous work. These master alloys would then be added to a steel melt and poured into plate test castings for mechanical and metallurgical testing to ensure grain refinement occurs.

References

1. Zrnik, J., Kvackaj, T., Sripinproach, D., Sricharoenchai, P., "Influence of Plastic Deformation Conditions on Structure Evolution in Nb-Ti Microalloyed Steel," *Journal of Materials Processing Technology*, Vol. 133, No. 1-2, pp. 236-242, 2003.
2. Lottey, K. R., Militzer, M., "Microstructure Evolution in Fine-grained Microalloyed Steels," *Materials Science Forum*, pp. 347-354, 2005.
3. Ghosh, A., Das, S., Chatterjee, S., "Ultrahigh Strength Hot Rolled Microalloyed Steel: Microstructure and Properties," *Materials Science and Technology*, Vol. 21, No. 3, pp. 325-333, 2005.
4. Peter, J., Peaslee, K. D., Panda, D., "Thermomechanical Processing of HSLA Wide-flange Steel Beams for Increased Core Roughness," *Iron & Steel Technology*, Vol. 1, No. 7, pp. 172-180, 2004.
5. Fernandez, J., Illescas, S., Guilemany, J. M., "Effect of Microalloying Elements on the Austenitic Grain Growth in a Low Carbon HSLA Steel," *Materials Letters*, Vol. 61, No. 11-12, pp. 2389-2392, 2007.
6. Chen, G., Yang, W., Guo, S., Sun, Z., "Characteristics of Microstructural Evolution During Deformation-enhanced Ferrite Transformation in Nb-microalloyed HSLA Steel," *Journal of University of Science and Technology Beijing*, Vol. 14, No. 1, pp. 36-40, 2007.
7. Kang, J. S., Huang, Y., Lee, C. W., Park, C. G., "Effect of Thermo-mechanical Process on the Microstructure and Mechanical Properties of Low Carbon HSLA Steels," *Advanced Materials Research*, Vol. 15-17, pp. 786-791, 2007.

8. Chakrabarti, D., Davis, C., Strangwood, M., "Characterization of Bimodal Grain Structures in HSLA Steels," *Materials Characterization*, Vol. 58, No. 5, pp. 423-438, 2007.
9. Timokhina, I. B., Hodgson, P. D., Ringer, S. P., Zheng, R. K., Pereloma, E. V., "Precipitate Characterization of an Advanced High-strength Low-alloy (HSLA) Steel Using Atom Probe Tomography," *Scripta Materialia*, Vol. 56, No. 7, pp. 601-604, 2007.
10. Hotta, S., Murakami, T., Narushima, T., Iguchi, Y., Ouchi, C., "Effects of Cooling Rate and Direct Hot Deformation Conditions After Solidification on the Austenitic Microstructure Evolved by Simulated Strip Casting and Thin Slab Casting Processes in HSLA Steels," *Advanced Materials Research*, Vol. 15-17, pp. 726-731, 2007.
11. Chen, Y. T., Guo, A. M., Wu, L. X., Zeng, J., Li, P. H., "Microstructure and Mechanical Property Development in the Simulated Heat Affected Zone of V Treated HSLA Steels," *Acta Metallurgica Sinica*, Vol. 19, No. 1, pp. 57-67, 2006.
12. Megahed, G., Paul, S. K., Carboni, A., Pigani, A., Piemonte, C., "The Development of New Steel Grades and Products: Casting and Rolling of APIX70 Grades for Arctic Applications in a Thin Slab Rolling Plant," *Proceedings of the McMaster Symposium on Iron & Steelmaking*, Vol. 33, pp. 292-300, 2005.
13. Alvarez, P., Lesch, C., Bleck, W., Petitgand, H., Schottler, J., Sevillano, J. G., "Grain Refinement of Rapid Transformation Annealing of Cold Rolled Low Carbon Steels," *Materials Science Forum*, Vol. 500, pp. 771-778, 2005.
14. Lottey, K. R., Militzer, M., "Microstructure Evolution in Fine-grained Microalloyed Steels," *Materials Science Forum*, Vol. 500, pp. 347-354, 2005.
15. Zarandi, F., Yue, S., "Improvement of Hot Ductility in the Nb-microalloyed Steel by High Temperature Deformation," *ISIJ International*, Vol. 45, No. 5, pp. 686-693, 2005.
16. Khoo, C. A., Fourlaris, G., "Control of Grain Size by Second Phase Particle Additions in Novel HSLA Strip Steels," *Material Science & Technology 2004*, Vol. 1, pp. 21-29, 2004.
17. Gao, W., Garcia, C. I., DeArdo, A. J., "The Nucleation of Ferrite from a Coarse Grained Austenite During the Slow Continuous Cooling of an HSLA Steel," *Mechanical Working and Steel Processing Conference Proceedings*, Vol. 41, pp. 243-256, 2003.
18. Zhao, X. M., Wu, D., Zhang, L. Z., Liu, Z. Y., "Modeling of Isothermal Precipitation Kinetics in HSLA Steels and its Application," *Acta Metallurgica Sinica*, Vol. 17, No. 6, pp. 902-906, 2004.
19. Beres, M., Weirich, T., Hulka, K., Mayer, J., "TEM Investigations of Fine Niobium Precipitates in HSLA Steel," *Steel Research International*, Vol. 75, No. 11, pp. 753-758, 2004.
20. Peter, J., Peaslee, K., Panda, D., "Thermomechanical Processing of HSLA Wide-flange Steel Beams for Increased Core Toughness," *Iron & Steel Technology*, Vol. 1, No. 7, pp. 172-180, 2004.
21. Bramfitt, B., "The Effect of Carbide and Nitride Additions on the Heterogeneous Nucleation Behavior of Liquid Iron," *Metallurgrical Transactions*, Vol. 1, pp. 1987-1995, 1979.
22. Easton, M., St. John, D. H., "Grain Refinement of Aluminum Alloys: Part II. Confirmation of, and a Mechanism for, the Solute Paradigm," *Metallurgical and Materials Transactions A*, Vol 30A, pp. 1625-1633A, 1999.
23. Mohanty, P. S., Gruzleski, J. E., "Mechanism of Grain Refinement in Aluminum," *Acta Metallurgica Materialia*, Vol. 43, No. 5, pp. 2001-2012, 1995.
24. Kearns, M. A., Cooper, P. S., "Effects of Solutes on Grain Refinement of Selected Wrought Aluminum Alloys," *Materials Science and Technology*, Vol. 13, No. 8, pp. 650-654, 1997.
25. Xu, H., Xu, L. D., Zhang, S. J., Han, Q., "Effect of the Alloy Composition on the Grain Refinement of Aluminum Alloys," *Scripta Materialia*, Vol. 54, No. 12, pp. 2191-2196, 2006.
26. Iqbal, N., van Dijk, N. H., Hansen, T., Katgerman, L., Kearley, G. J., "The Role of Solute Titanium and TiB2 Particles in the Liquid-solid Phase Transformation of Aluminum Alloys," *Materials Science & Engineering, A: Structural Materials: Properties, Microstructure and Processing*, Vol. A386, No. 1-2, pp. 20-26, 2004.

27. Quested, T. E., Greer, A. L., "The Effect of the Size Distribution of Inoculant Particles on As-cast Grain Size in Aluminium Alloys," *Acta Materialia*, Vol. 52, No. 13, pp. 3859-3868, 2004.
28. Easton, M., St. John, D. H., "Factors Affecting the Development of a Fine Grained Solidification Microstructure in Aluminum Alloys," *Proceedings of a Symposium held during the TMS Annual Meeting*, Charlotte, NC, Mar. 14-18, 2004, pp. 147-156, 2004.
29. Lee, Y. C., Dahle, A. K., St. John, D. H., "The Role of Solute in Grain Refinement of Magnesium," *Metallurgical and Materials Transactions A: Physical Metallurgy and Materials Science*, Vol. 31A, No. 11, pp. 2895-2906, 2000.
30. Dahle, A. K., Arnberg, L., "On the Assumption of an Additive Effect of Solute Elements in Dendrite Growth," *Materials Science & Engineering, A: Structural Materials: Properties, Microstructure and Processing*, Vol. A225, No. 1-2, pp. 38-46, 1997.
31. Spittle, J. A., Sadli, S., "Effect of Alloy Variables on Grain Refinement of Binary Aluminum Alloys with Al-Ti-B," *Materials Science and Technology*, Vol. 11, No. 6, pp. 533-537, 1995.
32. Backerud, L., "Grain Refining Mechanism in Aluminum-titanium-boron Alloys," *Jernkontorets Annaler*, Vol. 155, No. 8, pp. 422-424, 1971.
33. Moore, J. J., "Rare Earth Desulphurization of Sand Cast Steel," *The British Foundryman*, Vol. 75, No. 10, pp. 173-182, 1982.
34. Li, H., McLean, A., Rutter, J. W., Sommerville, I. D., "Influence of Rare Earth Metals on the Nucleation and Solidification Behavior of Iron and 1045 Steel," *Metallurgical Transactions B*, Vol. 19B, pp. 383-395, 1988.
35. Qingxiang, Y., Xuejun, R., Bo, L., Mei, Y., Xin, W., "Discussion of RE Inclusions as Heterogenous Nuclei of Primary Austenite in Hardfacing Metals of Medium-High Carbon Steels," *Journal of Rare Earths*, Vol. 17, No. 4, pp. 293-297, 1999.
36. Guo, M., and Suito, H., "Influence of Dissolved Cerium and Primary Inclusion Particles of Ce_2O_3 and CeS on Solidification Behavior of Fe-0.2 mass%C-0.02 mass%P Alloy," *ISIJ International*, Vol. 39, No. 7, pp. 722-729, 1999.
37. Lan, J., Junjie, H., Wenjiang, D., Qudong, W., Yanping, Z., "Effect of Rare Earth Metals on the Microstructure and Impact Thoughness of a Cast 0.4C-1.2Mo-1.0V Steel," *ISIJ International*, Vol. 40, No. 12, pp. 1275-1282, 2000.
38. Van der Eijk, C., Walmsley, J., "Grain Refinement of Fully Austenitic Stainless Steels Using a Fe-Cr-Si-Ce Master Alloy," *Proceedings of the 59th Electric Furnace Conference*, pp. 51-60, November 2001.

Progress Statement Summary

All of the originally proposed project tasks were completed, plus two additional tasks in a no cost project extension. A review of the current literature (Task 1) on the grain refinement of steels provided a good basis for the experiments planned as part of this project. Task 2 was to conduct a series of experiments on rare earth additions to carbon steels. Two sets of experiments were conducted under this task. The first set consisted of a set of plate castings with a rare earth (RE) silicide or Engineering Grain Refiner (EGR) addition to 1010 steel. This was done to determine the structure-property relationships with these additions. These experiments occurred under better molding sand control, which eliminated the porosity from the PI's previous ONR project. A second series of experiments were conducted with a high phosphorous content. This allowed the use of Oberhoffer's etch to determine the macrostructure of the steel. Examination of the macrostructure enabled the PI to determine if the RE silicide or EGR additions caused a change in the solidification of the steel. For Task 3, the PI conducted two different sets of phase equilibrium experiments. The first was only between higher purity CeO_2 and La_2O_3 powders and commercial refractories. The second set consisted of a steel pin of 1018 or 304 steel inside a commercial refractory with CeO_2 or La_2O_3 power. These experiments helped building an understanding of how commercial refractories reacted with the RE oxides. This investigation provided very basic information,

which was lacking in the open literature, on the governing thermodynamics. In Task 4, the PI conducted thermal analysis and differential scanning calorimetry (DSC) experiments to analyze the effect of RE additions on the eutectoid reaction in plain carbon steels. It was found that no changes in the A_1 or A_3 temperatures occurred with the addition of the RE silicide or EGR. For samples that were quenched and tempered and fifty percent increase in strength at the same ductility was observed for the steels treated with EGR. Due to the results of Task 4, Task 5 was not required as originally thought. Task 6 consisted of creating a series of master alloys and different addition methods in an attempt at improving the level of refinement. One series of experiments consisted of various method for improving the recovery of the RE silicide or EGR addition. While a second set of experiments focused on creating a new set of RE based master alloys. The PI also experimented with a TiC master alloy concept that was not part of the original project proposal. Task 7 consisted of using the various master alloys created in Task 6 in a set of plate casting experiments to help determine their effectiveness in refining the structure of the steel. Tasks 8 and 9 were not originally proposed as part of the project but were part of a no-cost extension. Task 8 consisted of creating a set of RE silicide refined plate castings. These were then sectioned and machined into raw plates for cold rolling to various degrees of cold work. The purpose of this task was to determine if the RE oxy-sulfides responsible for refinement would cause any complications in a wrought steel processing route. Task 9 was another series of master alloys created with a different technique. The master alloys were first created and then poured into plate castings for testing.

Progress

Task 1: Literature Review

The PI conducted a review of the literature on rare earth and non-rare earth based grain refinement. A bibliography was submitted to ONR as evidence that this was done.

Task 2: Experiments on Rare Earth Additions

. Rare earth additions have captured considerable research attention. Several questions remained unanswered during the previous project. The goal of the current project was to provide additional experimental data to answer those questions. The underlying mechanism at play has still not been fully elucidated by research to date. Also, there was inconsistent grain refinement observed during the previous experiments.

A series of plate castings were poured at three different rare earth addition rates. The plates are approximately 5.5 inches by 9 inches by 0.8 inches thick with a large 3 inch diameter, 3 inch tall riser. The gating system incorporates a 10 ppi filter at the bottom of the downsprue to remove inclusions. Computer simulations of the filling profile show a low turbulence filling pattern with a maximum in-gate velocity of 0.51 m/s. A 3 kHz induction furnace melted the 50 lb heats under an air atmosphere. At 3130°F, graphite, FeSi, and FeMn were added into the furnace and the melt tapped into a ladle. An aluminum shot addition during ladle filling fully deoxidized the steel. Rare earth additions were made by adding rare earth silicide in the ladle during the tap. Castings were poured at a 2920°F temperature. Prior to pouring, molds were manufacturing using a jolt/squeeze molding machine. The molding sand consisted of a 54 AFS GFN silica based molding sand that had 5% sodium bentonite (western bentonite) and 1.5% moisture content. After pouring, the castings cooled and were sectioned into metallurgical samples and tensile bars. Optical emission spectroscopy (OES) on a portion of the casting plate verified the chemical composition. Tensile testing was carried out by a local foundry in accordance with ASTM E8 using half inch diameter tensile bars.

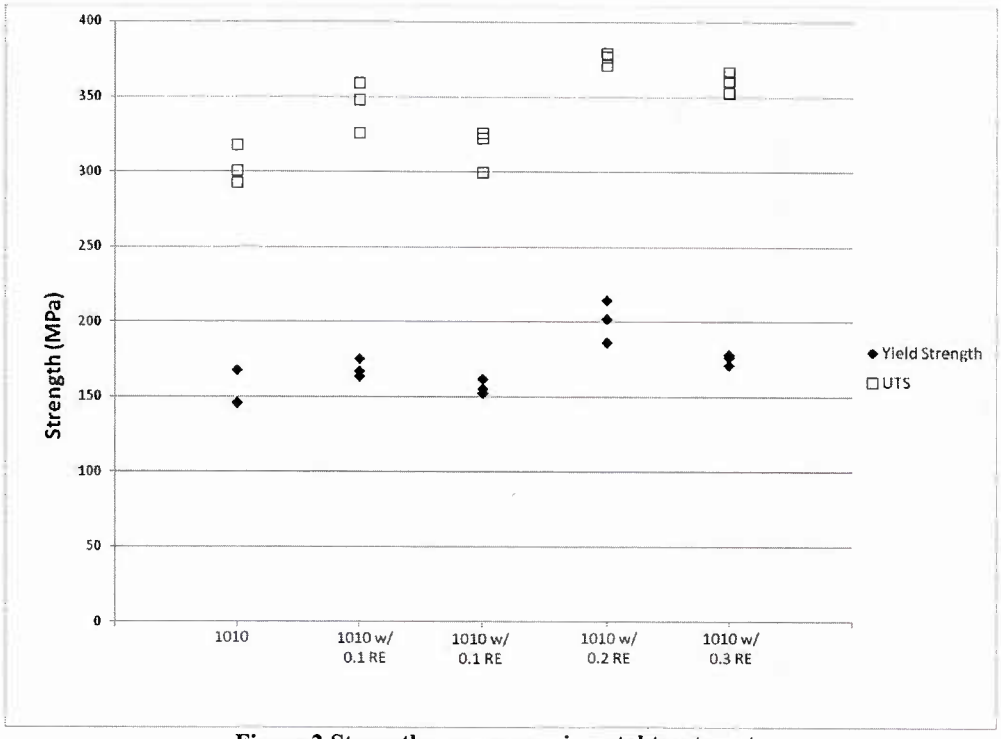

Figure 2 Strength verses experimental treatment.

Strength for some of the rare earth addition experimental heats was higher than the strength of the baseline material (See Figure 2). The average yield strength for the baseline heat was 153 MPa, while the average for the 0.1 RE, 0.2 RE, and 0.3 RE were 162 MPa, 200 MPa, and 175 MPa respectively. The average UTS for the baseline, 0.1 RE, 0.2 RE, and 0.3 RE were 304 MPa, 330 MPa, 376 MPa, and 360 MPa. Elongation was also higher for the rare earth containing heats (See Figure 3). The elongation data is higher for all heats compared to the baseline 1010 data. The PI would also like to note that this elongation data has less scatter and higher values than those from the previous project, which is likely due to the reduction in porosity caused by molding sand issues. The strength and elongation was also found to be a strong function of the cerium content of the steel. (The SVSU OES spectrometer was only calibrated to measure cerium content due to limited certified reference materials (CRMs) for rare earth content in iron matrices.) Significant strengthening occurred when the actual cerium content was approximately 0.0012% (See Figure 4). Elongation dramatically improved above 0.004% Ce and also peaked above 0.0012% Ce (See Figure 5). The data presented in Figures 4 and 5 are consistent with a heterogeneous nucleation model since an increasing amount of nuclei are formed with higher alloy additions. The data suggests that there is a minimum cerium content required to achieve significant strengthening. Microstructural observation found that the grain size of the rare earth containing samples was smaller than the baseline steel. The average linear intercept grain size for the baseline material was 125 μm while the average for all rare earth samples was 110 μm. Unfortunately, it was not possible to find a statistically significant difference in the grain size due to large variation in the linear intercept grain size measurements.

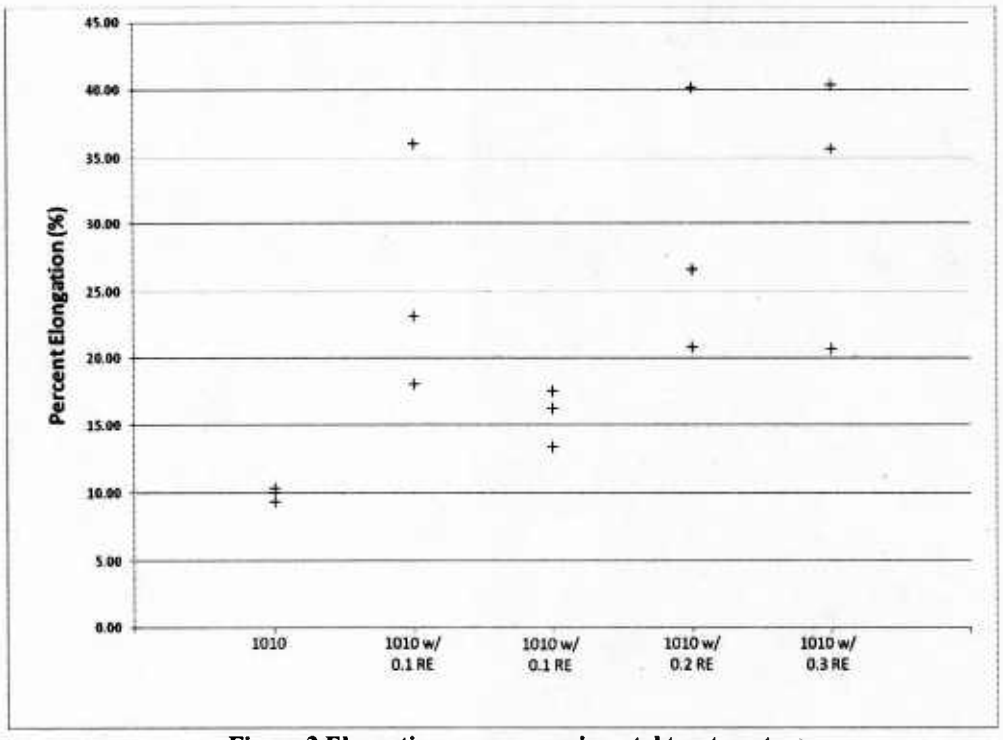

Figure 3 Elongation verses experimental treatment.

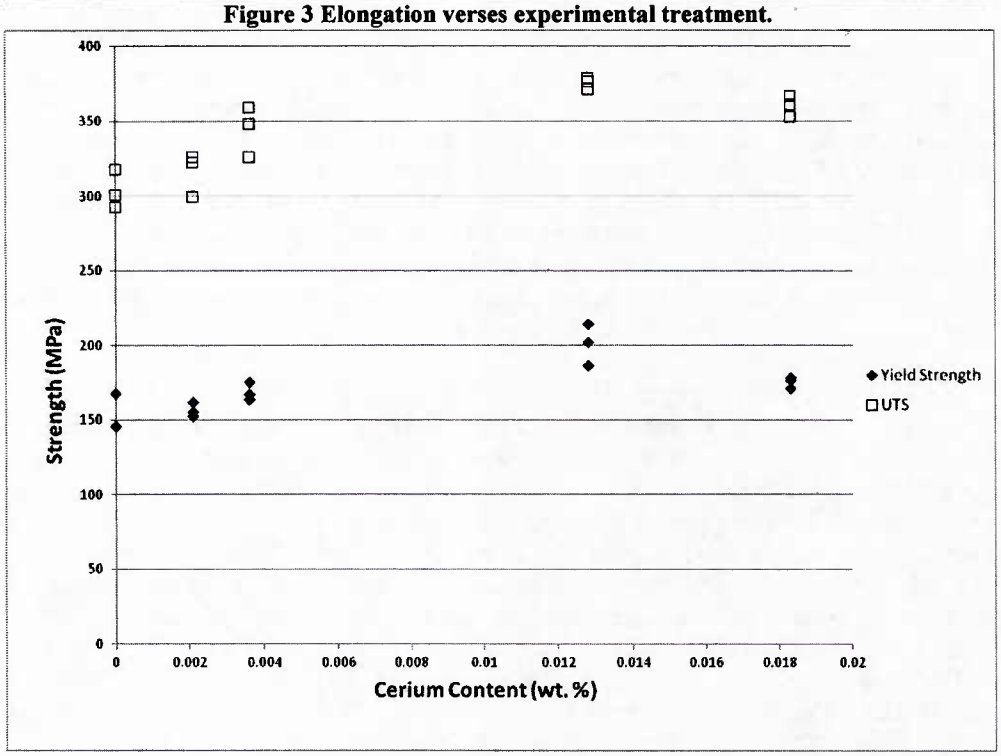

Figure 4 Strength verses actual cerium content.

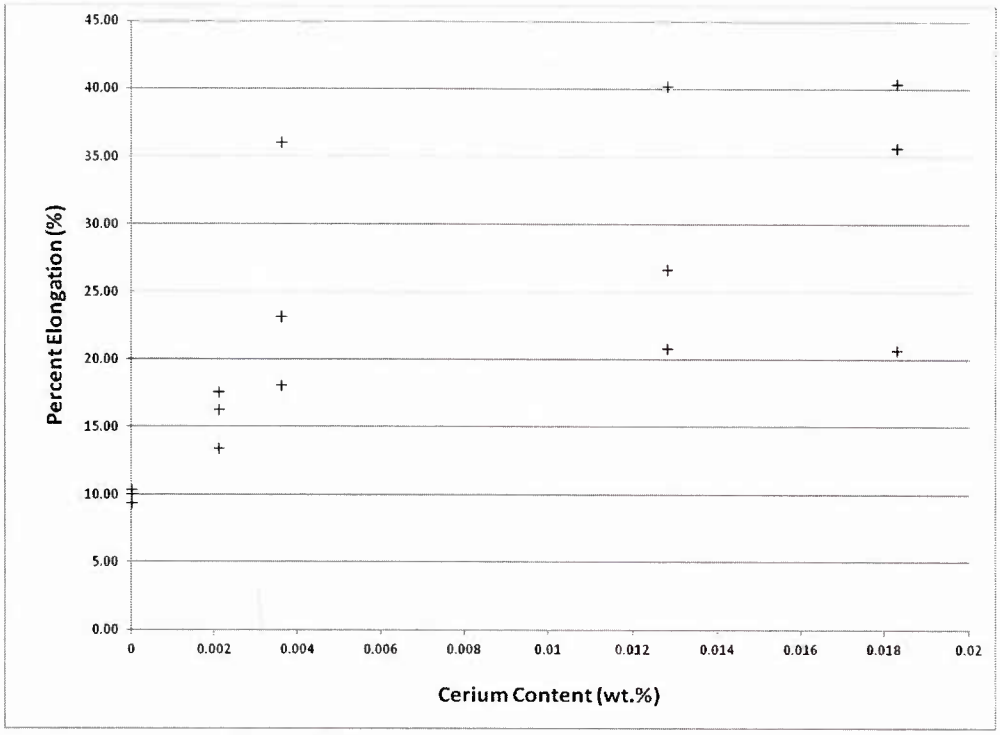

Figure 5 Elongation verses actual cerium content.

Electron microscopy of the samples observed a significant number of rare earth oxides within the microstructure. Energy dispersive spectroscopy (EDS) in SVSU's scanning electron microscope (SEM) indicated complex rare earth- aluminum oxides formed in many of the rare earth containing heats. These oxides were typically 1-5 μm in size. Very few oxides were found with an oxide coating on them. One interesting observation was that the composition of the oxides changed as the rare earth content increased. Inclusions from the 0.1 RE sample had approximately a 15% rare earth content, while the inclusions from the 0.2 RE and 0.3 RE samples had contents near 20% and 40% respectively. It would be expected that these differences in composition would result in different crystal structures and may indicate why strengthening and grain size changes are strongly dependent on rare earth content.

The PI became aware that a proprietary grain refining alloy has been developed by a ferroalloy producer. The ferroalloy producer provided a sample of their alloy for experimentation. Plate castings with three different levels of this refiner were poured using the same process as the castings that had rare earth silicide added to them. Addition levels of 0.1%, 0.2%, and 0.3% were done to determine the effect of this refining alloy. Strength increased slightly upon the addition of this refiner (See Figure 6). The yield strength modestly increased from the baseline properties; however, the UTS showed a larger increase. The reason for this moderate increase may be the low cerium content of the steel (See Figure 7). All of the refining alloy additions produced approximately the same cerium content. This content is similar to the actual cerium content of the 0.1 RE samples manufactured in previous experiments by the PI. Those samples and these have similar (~ 168 MPa) yield strengths and UTS (~ 348 MPa). The refiner alloy additions resulted in a finer grain size than the baseline material. The measured liner intercept grain size for the baseline was 125 μm, while the refiner alloy addition samples had an average of 110 μm.

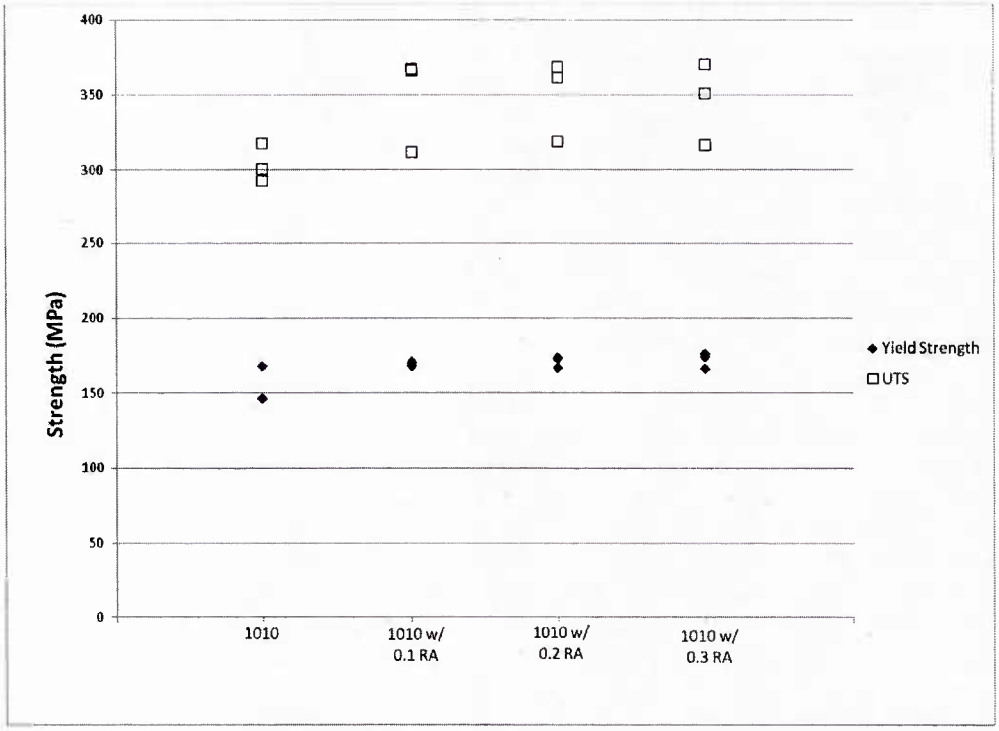

Figure 6 Effect of refiner alloy (RA) on strength.

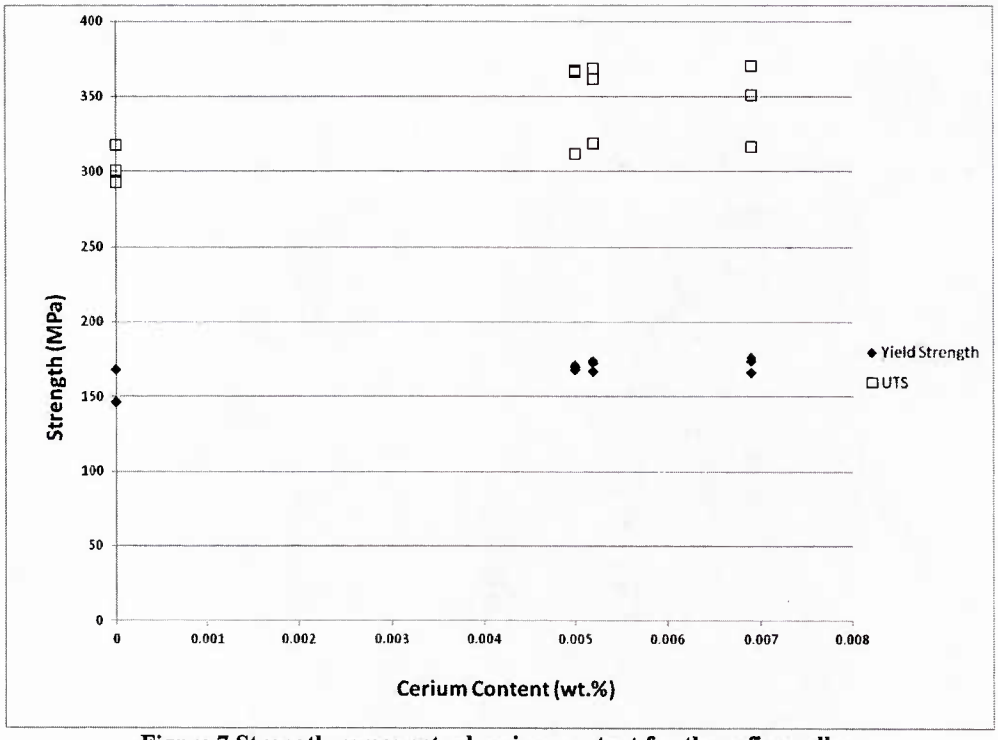

Figure 7 Strength verses actual cerium content for the refiner alloy.

The mechanism by which rare earth additions reduce grain size and improve properties has not been fully determined. The theory the PI has been using is that the rare earth oxides that form are effective nuclei for assisting the formation of solid steel during solidification. The introduction of a large number of these oxides/nuclei results in a decrease in grain size with a concurrent increase in strength. The difficulty with this theory is that the crystallographic structure of most of the rare earth oxides best match the FCC structure of austenite. Since 1010 and other plain carbon steels solidify as delta-ferrite initially, the postulated theory does not match this fact. Several paper reviewers have suggested to the PI that the rare earth oxides might instead assist nucleation of austenite during the solid state peritectic reaction and therefore create a smaller austenite grain size that later results in a smaller room temperature structure. This second mechanism would also result in many of the same experimental observations as the completely solidification based route propose by the PI.

To determine if the addition of rare earth elements affects steel solidification, the PI conducted experiments with high phosphorous levels (0.5%). As is generally known, high phosphorous levels are detrimental to steel properties; however, these levels enabled the PI to use Oberhoffer's etch (500 mL H_2O, 500 mL ethanol, 1g $CuCl_2$, 30 g FeCl, 50 mL HCl, and 0.5 g $SnCl_2$) to reveal the as solidified structure. Oberhoffer's etch preferentially etches phosphorous rich regions which form due to segregation during freezing. The PI employed this approach since the first phase to form is actually delta-ferrite and not austenite in plain carbon steels. Plate casting samples were cast utilizing the procedure outlined earlier in this report. FeP was added at 3130°F with the other alloying elements. Samples were polished in accordance with standard metallographic practice for steels and then imaged with a stereomicroscope.

A columnar microstructure was observed in several of the baseline 1010 samples (See Figure 8). Almost no equiaxed grains were observed. Samples containing 0.1 RE still had a columnar structure, but the length of the primary dendrites appeared to decrease (See Figure 9). An equiaxed region was observed in all the samples examined from the 0.2 RE material. The dramatic appearance of the equiaxed zone at this level would only occur if the rare earth addition modified the solidification of the alloy. If the rare earth oxides only assisted the formation of austenite within the solid then there should be no effect on the solidified structure. These relatively simple experiments support the PIs hypothesis that rare earth additions have an effect on steel solidification.

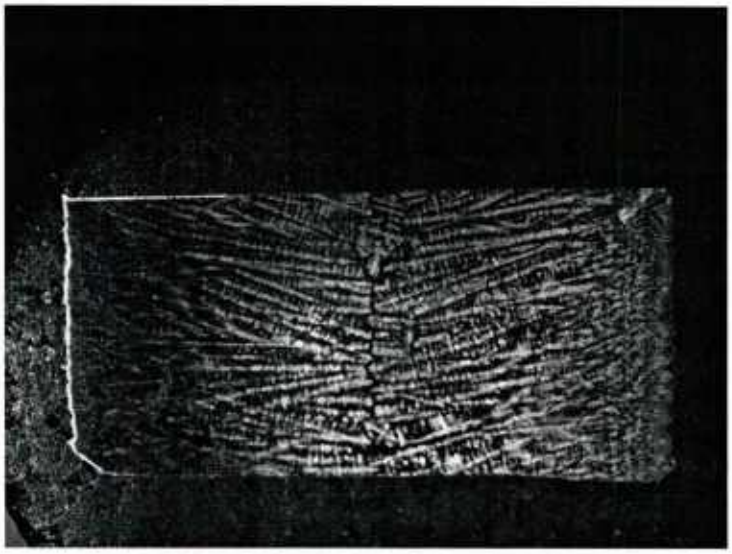

Figure 8 Micrograph from baseline 1010 with high P.

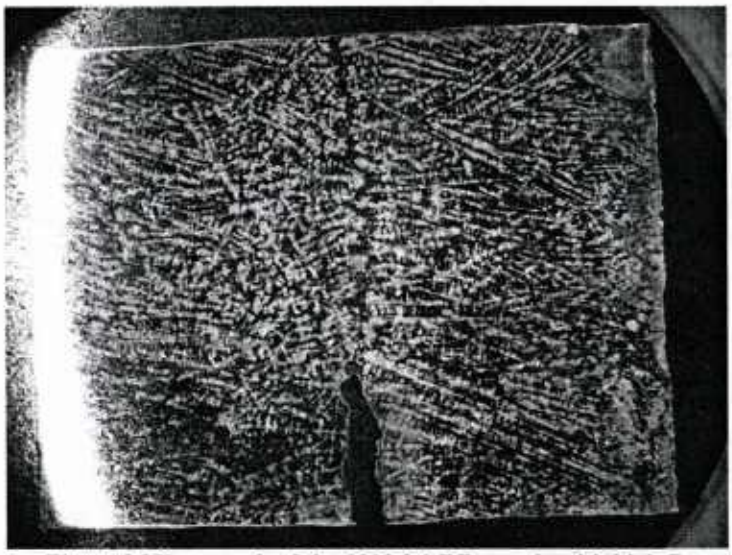

Figure 9 Micrograph of the 1010 0.1 RE sample with high P.

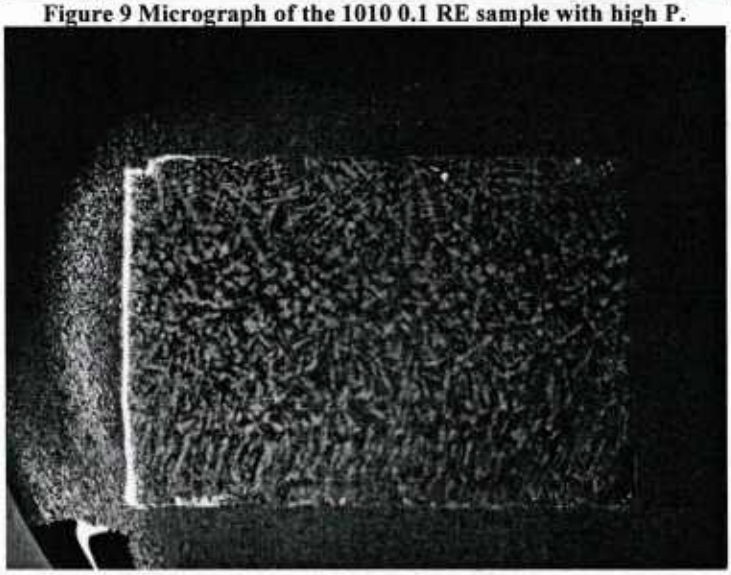

Figure 10 Micrograph of the 0.2 RE 1010 sample with high P.

Task 3: RE Oxide Phase Equilibrium Experiments

In the previous project, the PI observed that the rare earth oxides from steels that contained rare earth additions which did not produce refinement often contained rare earth oxides that were coated with an iron-aluminum oxide coating. This coating prevented the surface of the rare earth oxide from contacting the steel and effectively poisoned the nuclei. The PI postulated that the iron-aluminum oxide coatings had two sources. One was that the oxides were simply due to reoxidation of the steel during tapping that then coated the rare earth oxides. The other was that a refractory-inclusion reaction might occur in the melt.

Samples of 90%, 70%, and 50% alumina bricks commonly used by steel foundries were acquired. The major impurity phase in these bricks was silica (See Table 1). The bricks were sectioned into smaller samples for experimentation. A 99% pure alumina sample was pressed from 99% pure, -325 mesh

powder. This sample was fired prior to the phase equilibrium experiment. CeO_2 and La_2O_3 pucks made from 99% pure, -325 powders were pressed into 0.25 inch diameter pucks. These green pucks were placed on the test refractory samples (See Figure 11). A resistance furnace was heated at a rate of 2°C/min until 1590°C was attained. At 1590°C a three hour hold in air allowed the test refractories and RE oxides to react. The furnace cooled at 2°C/min to room temperature.

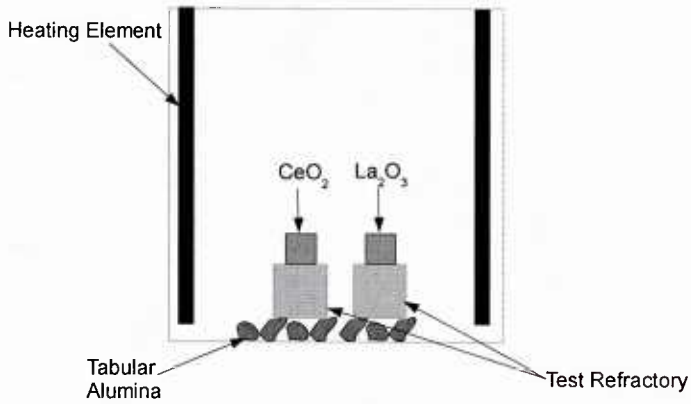

Figure 11 Schematic depiction of the phase equilibrium experimental setup.

Sample	Al_2O_3 (wt. %)	SiO_2 (wt. %)	Fe_2O_3 (wt. %)	TiO2 (wt. %)	CaO (wt. %)	MgO (wt. %)
99 % Alumina Puck	99	-	-	-	-	-
90% Alumina Brick	90.2	9.6	-	-	0.1	
70% Alumina Brick	69.4	24.3	1.7	3.2	0.3	0.4
50% Alumina Brick	42.2	52.6	1.4	2.3	0.2	0.3

Table 1 Composition of refractory materials

The 99% alumina and 90% alumina samples showed no signs of reaction with either CeO_2 or La_2O_3. However, the 70% alumina sample had some indications of a reaction between the refractory and CeO_2. A cerium rich alumino-silicate was found to have precipitated at the grain boundary of the refractory aggregate (See Figure 12). This reaction was limited to a 100 μm thick region at the interface of the two ceramics. The 50% alumina samples had a severe reaction with both rare earth oxides (See Figure 13). A low melting point phase formed. Almost half of the 50% alumina samples melted during the experiment. This sever reaction indicates that low alumina refractories should not be used with rare earth based grain refinement. SEM investigation of these samples revealed a rare earth rich silicate formed upon cooling to room temperature in the refractory that remained.

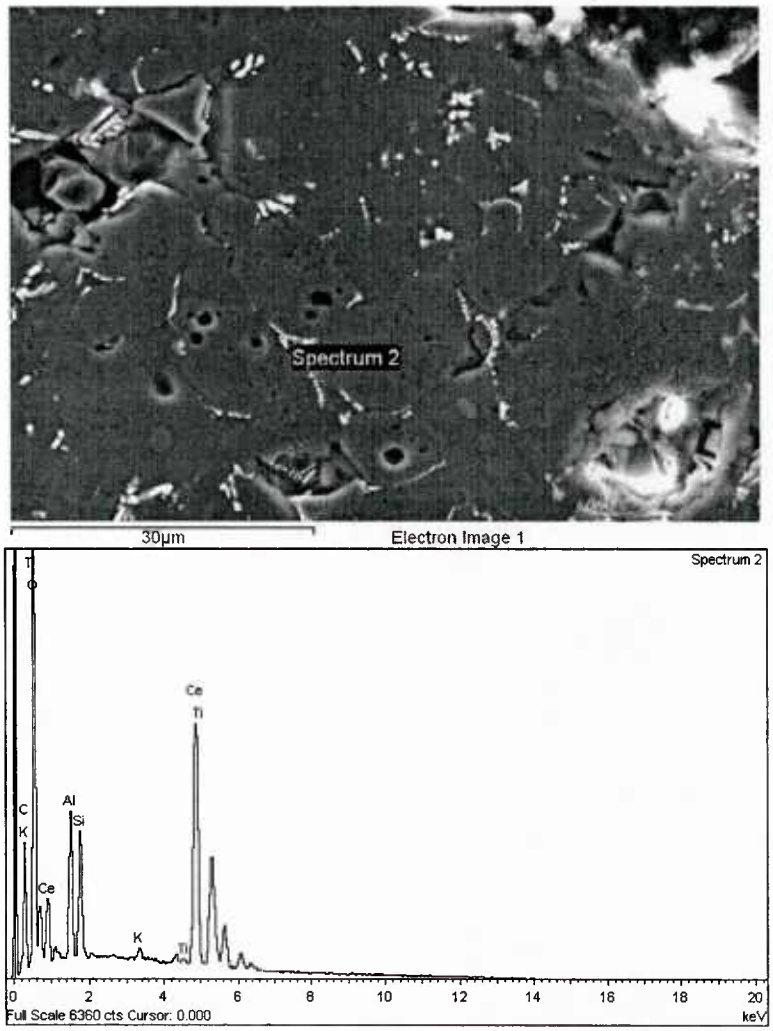

Figure 12 SEM micrograph and EDS spectra from RE rich oxide phase in 70% alumina brick exposed to CeO_2.

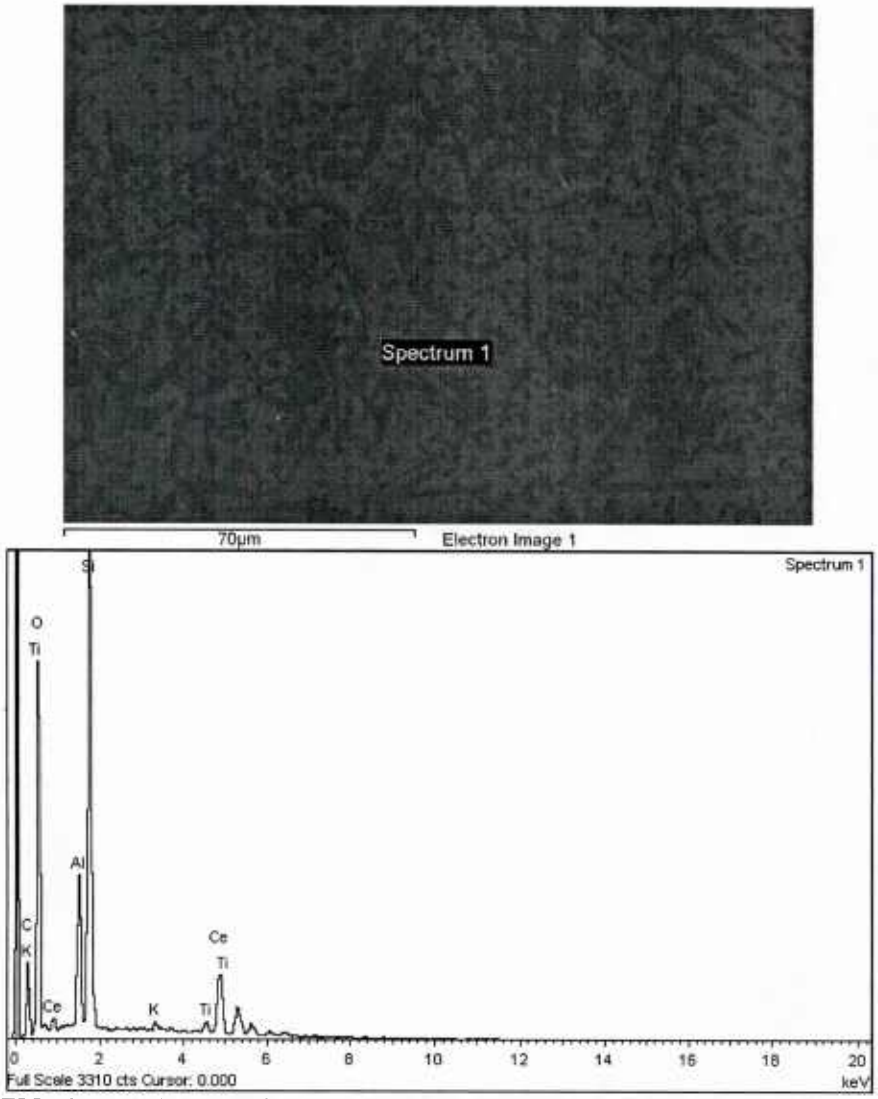

Figure 13 SEM micrograph and EDS spectra from RE rich oxide phase in 50% alumina brick exposed to CeO_2.

In addition to the previous experiments, a set of refractory pin experiments were conducted to provide data on the phase equilibrium between RE oxides, industrial refractories, and steel. Industrial refractories containing 90%, 70%, and 50% alumina were sectioned into pieces approximately 1in. x 2.5 in. x 2.25 in. A core drill drilled two 0.25 in. diameter, 1 in. deep holes into the refractory. For each refractory, a baseline, 0.25 g CeO_2, and 0.25g La_2O_3 test was done with 1018 and 304 stainless steel pins. The oxide powders were placed at the bottom of the hole with a precut steel pin placed on top.

The refractory/steel pin assembly was placed inside a larger alumina crucible that was filled with graphite (See Figure 3). A small alumina cover on top of the steel pin refractory prevented the infiltration of graphite. The graphite prevented oxidation of the steel. A final alumina cover on top of the outer alumina crucible sealed the entire experimental setup. This was then placed inside a high temperature resistance furnace. The furnace heated the samples at a rate of 5°C/min. until 1590°C was achieved. The samples were held for two hours before cooling at 5°C/min. After the experiment, a diamond saw sectioned the

refractory into specimens suitable for cold mounting. These metallographic samples were then polished for optical and electron microscopy.

Figure 14 Outer alumina crucible with graphite and test refractory inside.

The experiments in 1018 and 304 found a significant level of reaction between the RE oxides and the 50% alumina refractory. This was immediately obvious during sectioning since the bottom of the hole no longer had a rectangular geometry at the bottom, but a bulbous geometry. Such geometry indicates significant liquid phase formation at the experimental temperature. SEM/EDS examination of the samples found that a two phase alumino-silicate/RE-silicate compound formed. In the La_2O_3 samples, this RE-silicate phase contained primarily lanthanum as the rare earth phase, while in the CeO_2 samples the phase contained cerium. Despite the difference in which elements were observed, the composition was very similar, indicating a similar reaction. Figure 16 depicts these two phases. Compositions from EDS analysis are in Tables 1 and 2. In the 1018 samples, no presence of iron was detected in the RE-silicate phase. While some chromium was noted in the RE-silicate phase in the 304 stainless samples. The chromium content did appear higher in the RE-silicate than the alumino-silicate phase (See Tables 2 and 3).

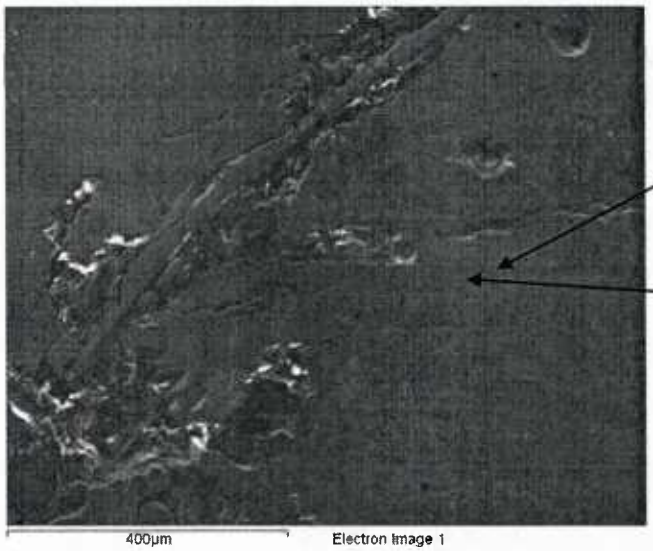

Figure 15 Refractory at the bottom of the pin in the 304 stainless steel-50% alumina sample with CeO_2.

Table 2 Quantitative EDS analysis of cerium silicate phase.

Element	Wt. %
O	45.28
Al	8.79
Si	22.84
Cr	9.85
Ce	13.24

Table 3 EDS analysis of the alumino silicate phase.

Element	Wt. %
C	8.13
O	49.67
Al	30.33
Si	9.46
Cr	2.40

The formation of a RE-silicate in equilibrium with an alumino-silicate phase is similar to the results reported earlier in this project. The only significant compositional difference occurred in the 304 stainless samples where chromium appears in both phases. The cerium-silicate contained more chromium than the lanthanum silicate. Reactions between the 90% and 70% alumina refractories were nonexistent. It appears that the reaction between the RE oxides is primarily with silica and not alumina. This makes sense with the composition of the RE-silicate phase identified. Due to the lower reaction amounts, it would be recommended that refractories containing at least 70% alumina be used when conducting grain refinement via RE additions. This will prevent excessive refractory erosion.

Task 4: Normalizing and Quench and Temper Heat Treatment Experiments on Grain Refined Steels

In the ori

Task 5: Experiments on Modifying Heat Treatments for Grain Refined Alloys

A series of thermal analysis experiments on 1010 and 1030 were conducted this fiscal year. Fifty pound heats of 1010 or 1030 were melted in a high frequency induction furnace. Once the initial charge of 1010 punchings melted and attained a temperature of 1720°C, FeSi, FeMn and graphite additions to the melt brought it to the desired composition. During tapping a final addition of aluminum shot and either rare earth (RE) silicide or Elkem Grain Refiner (EGR) occurred. Additions of RE silicide or EGR at target rare contents of 0 wt. %, 0.1 wt. %, and 0.3 wt. % were poured. After cooling to 1620°C in the ladle, the green sand molds of the plate casting were poured. The plate castings were sectioned into a metallographic, optical emission spectroscopy (OES), and thermal analysis (TA) samples (See Figure 16). The TA samples were one inch square, two inch tall with a 1/8 inch diameter hole (See Figure 16).

For the thermal analysis experiments themselves, an armored K-type thermocouple was placed inside the TA samples. It was cemented into place using high temperature cement. After the cement dried, the samples were placed in a furnace at 915°C for austenization. After being at 915°C for one hour after furnace recovery, the samples were removed and allowed to air cool. This procedure conforms to standard industrial practice. Temperature measurements were recorded at a rate of 2 Hz during the entire heat treatment. The heating and cooling curves and their first derivatives were examined to determine the A_1

and A_3 temperatures during heating and cooling. Three replicates per addition level were used. Figure 17 presents a typical heating curve and its derivative for a 1010 sample.

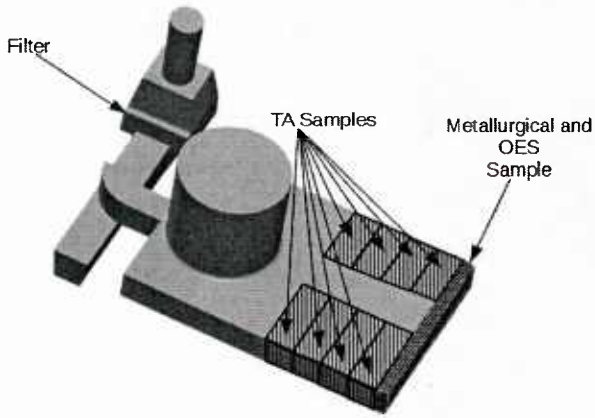

Plate Casting Thermal Analysis Sample Dimensions

Figure 16 Plate casting with sample locations depicted and the thermal analysis sample

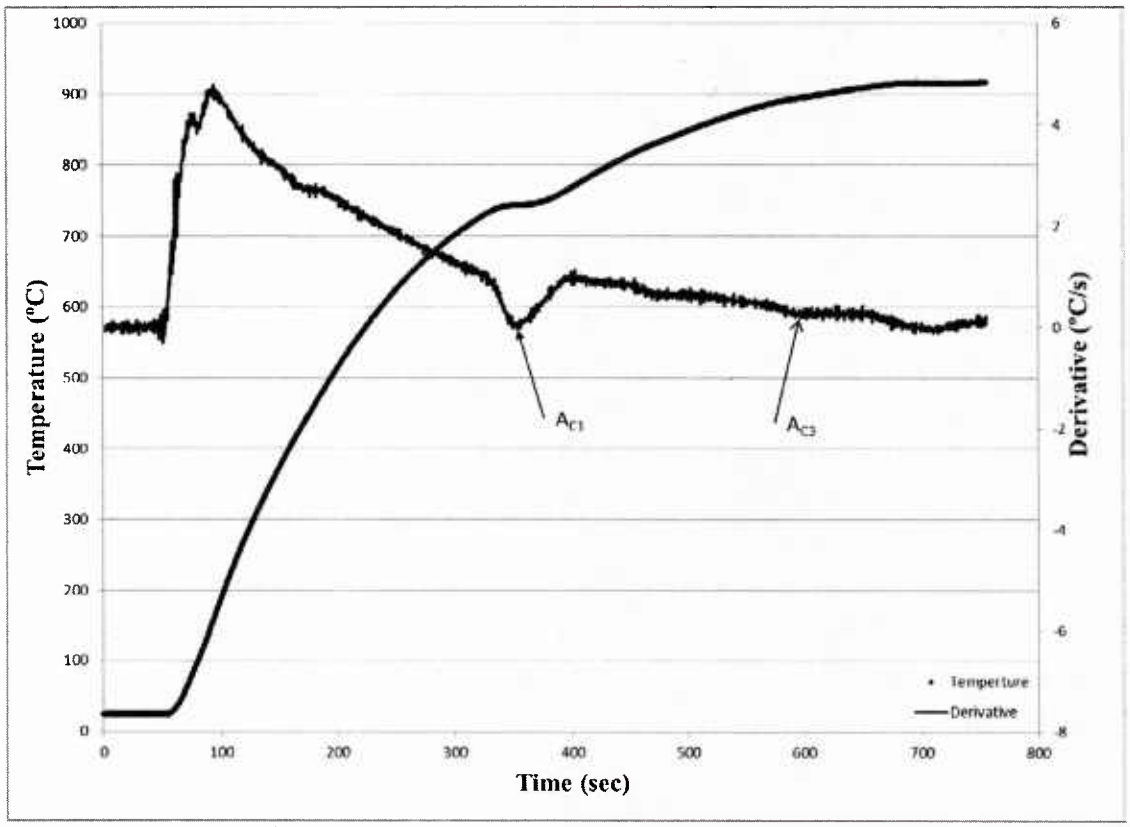

Figure 17 Typical heating curve from the 1010 baseline sample.

Table 5 lists the measured A_1 and A_3temperatures from the TA samples for 1010 and Table 6 presents the data from 1030. No significant differences in eutectoid reaction temperatures could be found between the baseline samples and any of the RE silicide or EGR samples. This would indicate that the addition of rare earth elements did not affect the eutectoid reactions significantly. There was one issued identified with

these experiments. ThermoCalc© predicted A_1 and A_3temperatures that were significantly different from the measured values. For the 1030, it predicted A_1 and A_3temperatures of 709°C and 814°C respectively. This discrepancy might be explained by the relatively high heating (5°C/s) and cooling rates (4°C/s) of the TA experiments. Rapid heating and cooling rates are known to make correct identification of phase reaction temperatures difficult.

Table 4 Eutectoid reaction temperatures for 1010.

Sample	Heating		Cooling	
	A_1 (°C)	A_3 (°C)	A_1 (°C)	A_3 (°C)
Baseline	742	890	662	796
0.1 RE	744	876	659	788
0.2 RE	743	884	660	791
0.3 RE	745	894	665	791
0.1 EGR	747	877	662	793
0.2 EGR	747	889	661	801
0.3 EGR	748	874	663	800

Table 5 Eutectoid reaction temperatures for 1010.

Sample	Heating		Cooling	
	A_1 (°C)	A_3 (°C)	A_1 (°C)	A_3 (°C)
Baseline	743	887	669	714
0.1 RE	746	872	674	703
0.2 RE	746	881	674	709
0.3 RE	746	893	671	718
0.1 EGR	746	883	669	711
0.2 EGR	746	881	674	715
0.3 EGR	752	890	668	701

While SVSU does not have a high temperature DSC, the PI was able to obtain access to an instrument at the University of Wisconsin-Milwaukee through Dr. Church. As-cast samples of 1030 from the TA experiments were sent for analysis. To reduce the effect of the heating and cooling rates upon A_1 and A_3 measurements, heating and cooling rates of 0.333°C/s were employed. The samples were heated to 1,000°C, held for ten minutes and then cooled while immersed in a 99.999% argon atmosphere. Table 6 lists the measured eutectoid reaction temperatures. There were no significant differences observed in the data. The measured A_1 and A_3 temperatures were actually quite close to those measured in the TA experiments. It would seem that the data in ThermoCalc's© database does not accurately predict the eutectoid reactions temperatures for the steel composition being employed.

Table 6 DSC measured eutectoid reaction temperatures for 1030 samples.

Sample	Heating		Cooling	
	A_1 (°C)	A_3 (°C)	A_1 (°C)	A_3 (°C)
Baseline	749	818	643	697
0.1 RE	749	831	647	687
0.2 RE	745	831	649	700
0.3 RE	747	834	648	696

Due to the small size of the TA samples, mechanical properties could not be tested which necessitated a separate set of tensile test castings to be poured. The melting and pouring procedures followed those outlined in the previous section. Rare earth silicide and EGR additions with target RE contents of 0 wt. % and 0.3 wt. % were used in these experiments. Two plates per heat were cast. One plate was sectioned into metallographic, OES, and tensile bar specimens in the as-cast state (See Figure 10). Tensile bar blanks were extracted from the second plate casting for normalizing. The tensile bar blanks were

normalized by being placed in a furnace at 915°C, being held for one hour after furnace recover, and then placed on a refractory brick and cooling in air. The tensile bars were then machined into 0.5 inch diameter tensile bars and tested on a hydraulic testing frame in accordance with ASTM E8. Free ferrite grain size measurements were also done using the procedure outlined in the previous section. Table 7 shows that the RE silicide and EGR sample had a finer microstructure than the baseline casting.

Table 7 Average ferrite grain size of the mechanical property castings in the as-cast condition.

Sample	Average Grain Size (μm)	95% Confidence Interval (μm)
Baseline	37	4.2
0.3 RE	30	5.5
0.3 EGR	28	4.9

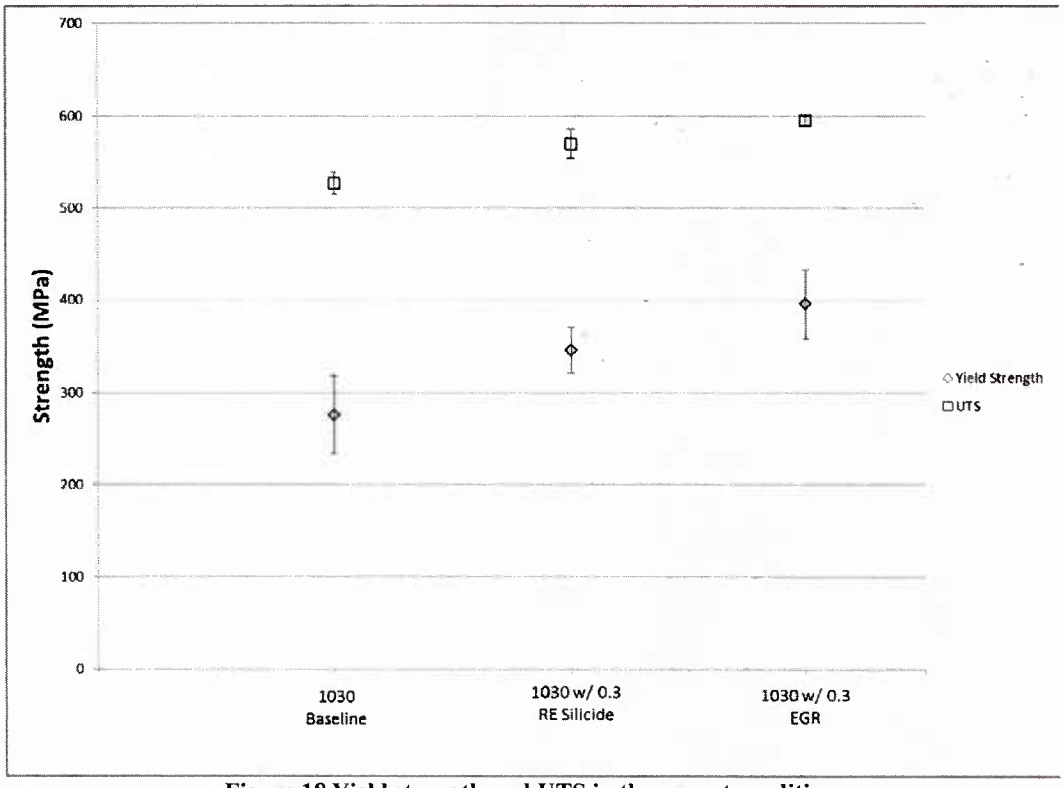

Figure 18 Yield strength and UTS in the as-cast condition.

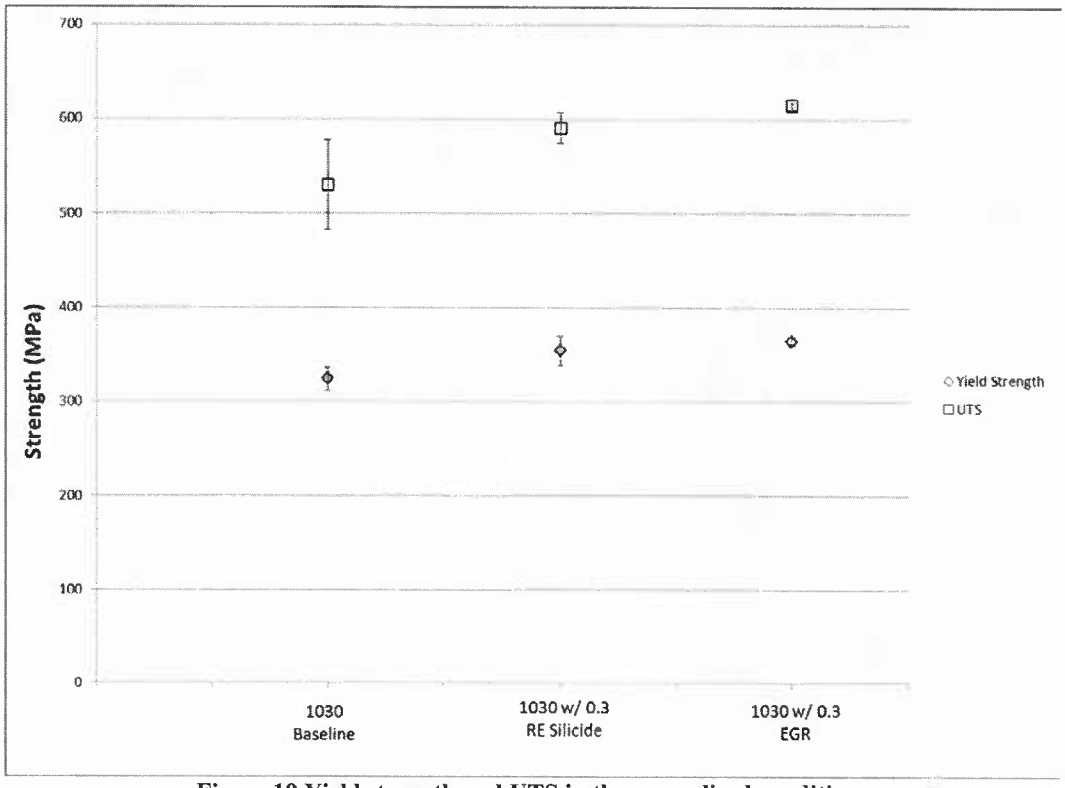

Figure 19 Yield strength and UTS in the normalized condition.

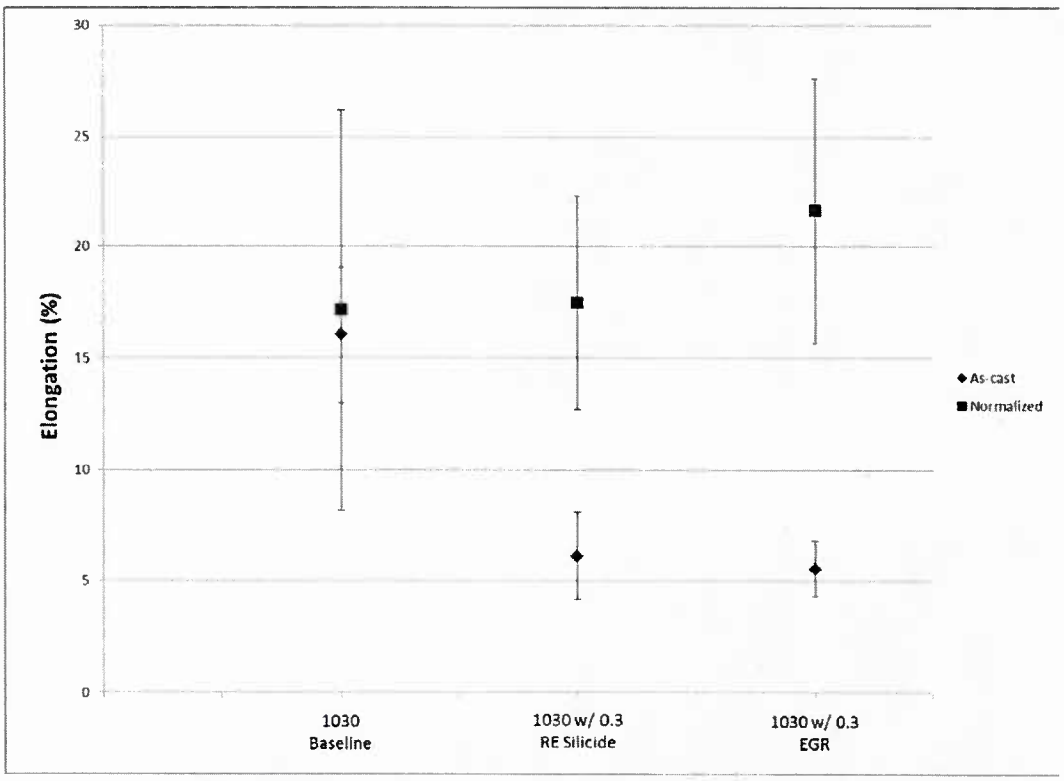

Figure 20 Elongation in the as-cast and normalized conditions.

The RE silicide and EGR samples had an average yield strength of 346 MPa and 395 MPa, respectively, in the as-cast condition (See Figure 18). This was statistically higher than the 275 MPa yield strength of the baseline samples. The ultimate tensile strength (UTS) was also statistically higher in the as-cast condition (See Figure 18). While the differences decreased slightly after normalization, the RE silicide and EGR samples still had statistically higher strengths (See Figure 19). More interesting was the elongation data. Prior to normalizing, the RE silicide and EGR samples had a much lower elongation. After normalizing, they had a higher elongation, although not statistically significant due to higher variation in the data. The as-cast elongations were unusually low for this steel. And the depicted trend was not expected since finer grain sizes typically produce higher elongations. Examination of the fracture surfaces found the presence of fish eyes on the as-cast samples. These indicate hydrogen embrittlement of the steel. Hydrogen embrittlement causes a sharp decrease in the ductility of steel and often has an associated increase in strength. It also explains why the elongation dramatically increased after normalizing. While austenitizing, the hydrogen within the tensile bar samples diffuses into the atmosphere and reduces the hydrogen content of the steel. Due to the lower hydrogen content, the normalized steels were not embrittled and therefore had higher elongations. No evidence of fish eyes were observed on any of the normalized bars, which supports the hydrogen embrittlement theory. The precise cause of the hydrogen was not determined, but could have been due to excess steam generated by the green sand molds during solidification.

To further examine the role of heat treatment in RE refined steels, tensile bars were also cast for quench and tempered heat treatment. Fifty pound heats of 1030 were melted in an induction furnace under an air atmosphere. One the heats reached 1720°C, ferroalloys and graphite were added prior to tapping. During tap, aluminum shot and either 0 wt. %, 0.1 wt. %, or 0.3 wt. % RE silicide or EGR were added. Two plate castings per heat were then poured in green sand molds. After cooling, one plate was sectioned to produce metallographic, OES, and tensile bar samples. Sectioning of the second plate created tensile bar samples

which were then quench and temper heat treated. These bars were austenitized at 860°C for one hour after furnace recovery and quenched in a 15°C water bath. This was followed by tempering at 400°C for half an hour after furnace recovery.

The microstructures in the Q&T contained minor amounts of free ferrite with mostly a tempered martensite structure (See Figure 21). The presence of free ferrite indicates that the cooling rate during quenching did not completely avoid the pearlite nose of the eutectoid reaction. Optically the structures of the baseline and 0.3 RE samples did not appear significantly different (See Figure 21A and 21B). However, the 0.3 EGR sample had considerable variations in the tempered martensite coloration (See Figure 6C). Qualitatively the free ferrite appears smaller in the 0.3 EGR sample than the baseline; yet, the author could not reliably quantify this due to issues in conducting image analysis on the images.

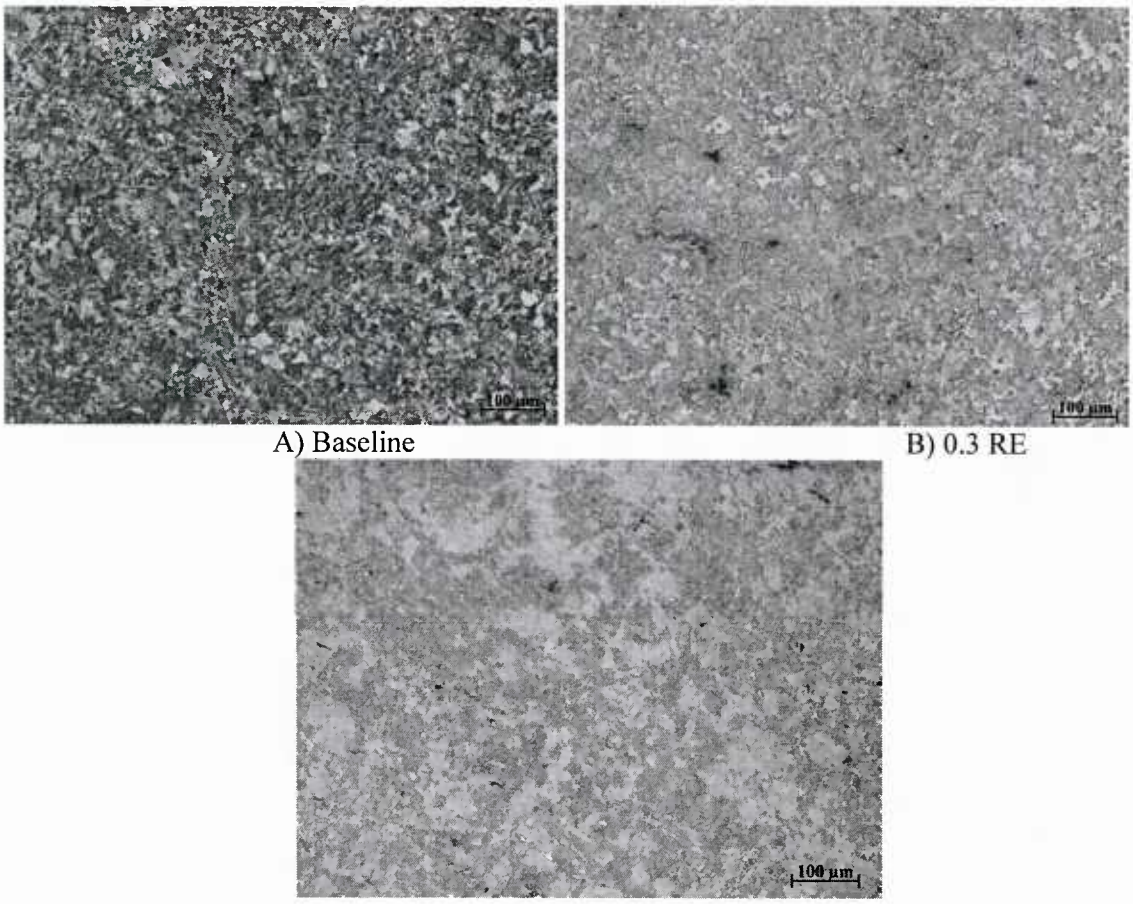

A) Baseline B) 0.3 RE

C) 0.3 EGR

Figure 21. Representative microstructures for the Q&T condition.

Mechanical testing of the Q&T plates in the as-cast and Q&T condition displayed very different trends from the normalized materials. In the as-cast state, the YS was statistically the same despite the 0.3 RE

samples having the highest average YS (See Figure 22). However, the treated steels had a higher UTS at 539 MPa for the 0.3 RE and 551 MPa for the 0.3 EGR samples verses the 486 MPa UTS of the baseline steel. This difference was statistically significant. The YS and UTS of the treated steels were significantly higher than the baseline material in the Q&T condition (See Figure 23). The average YS of the baseline, 0.3 RE, and 0.3 EGR were 606 MPa, 760 MPa, and 901 MPa respectively. The 0.3 RE and 0.3 EGR had YS 25% and 49% higher than the baseline. Average UTS for the baseline, 0.3 RE, and 0.3 EGR were 769 MPa, 915 MPa, and 982 MPa. This represents a 19% and 28% increase in UTS over the baseline for the 0.3 RE and 0.3 EGR samples respectively. All of the differences in strength were statistically significant. These strength increases are much higher than those observed in the normalized condition. It appears that, unlike the case with normalizing, there is a significant benefit to quench and tempering grain refined steels even when the strengths appear similar. The dramatically higher strengths of the treated steels, despite similar strengths in the as-cast condition, point to perhaps a continued role of the inclusions during heat treating.

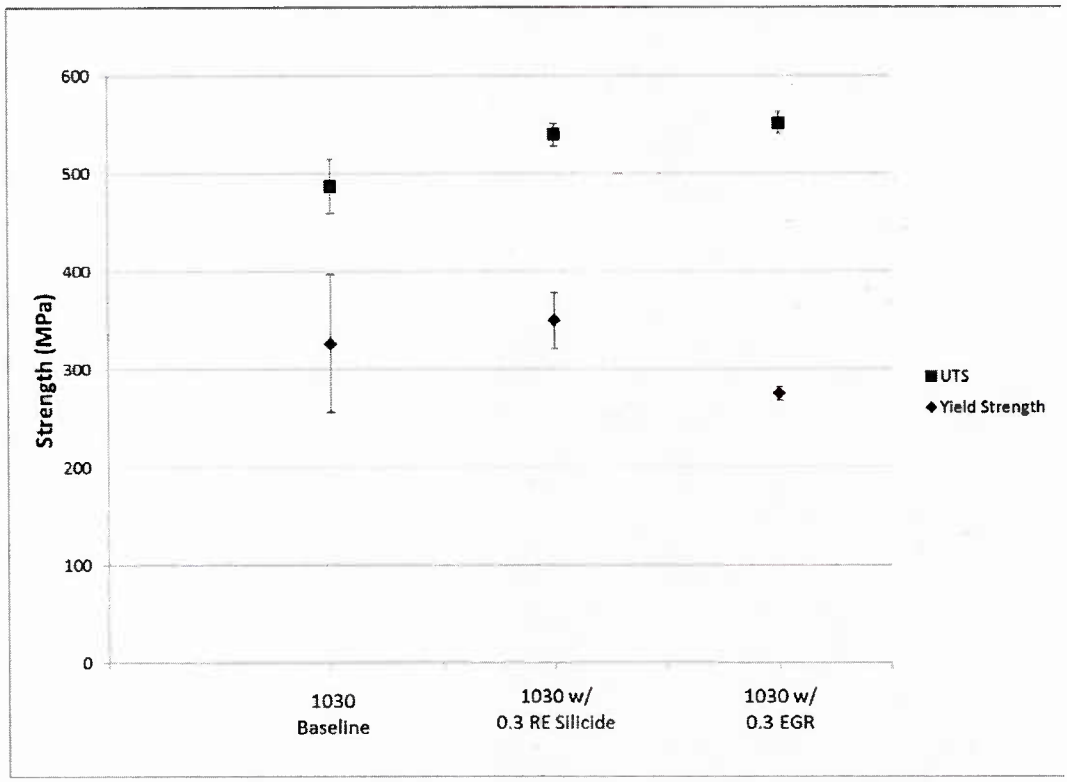

Figure 22. Mechanical properties of the Q&T plates in the as-cast condition.

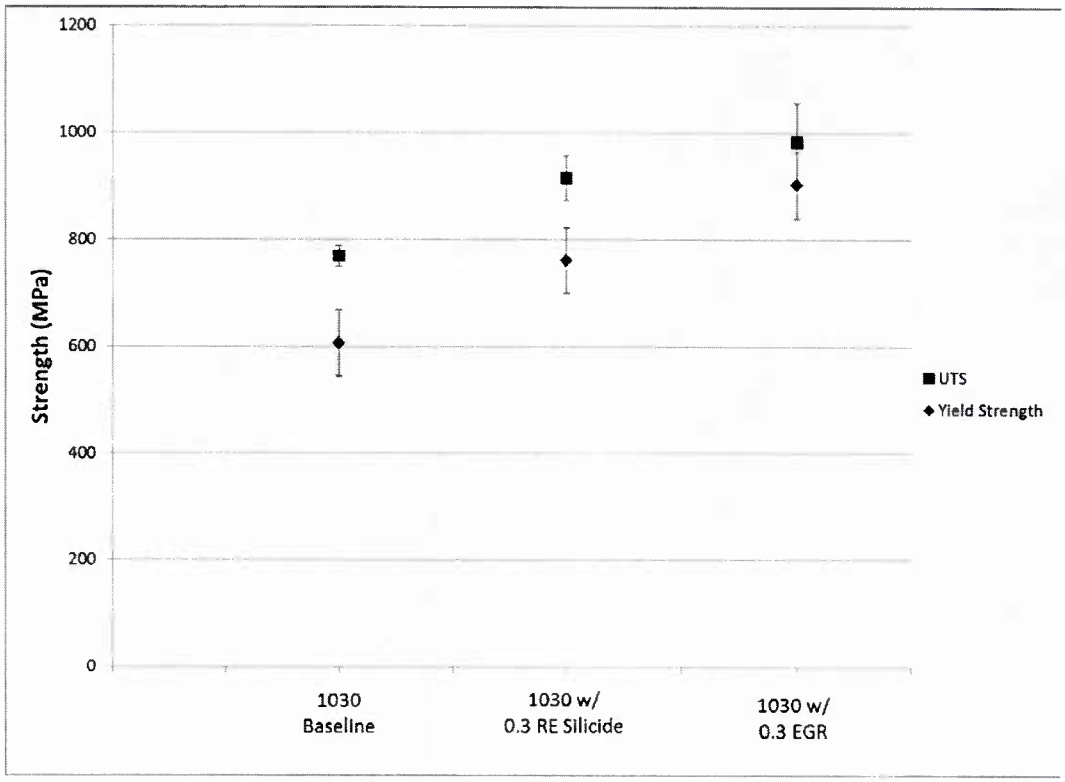

Figure 23. Mechanical properties in the Q&T condition.

Task 6: Creation of Rare Earth Based Master Alloy & Task 7: Structure-property Experiments with Rare Earth Master Alloy

Because of the interrelation of Tasks 6 and 7 they are being covered in one section. Several different attempts to create master alloys were done. These essentially broke down into three experimental series. One set primarily focused on changing the addition method to improve RE recovery. A second set created a TiC containing master alloy that was then added into steel to create plate castings for mechanical testing. The final series of experiments created RE based master alloys with different target inclusion compositions.

The addition method experiments used the same 25 mm by 127 mm by 250 mm plate casting employed in the previous experiments. Melting proceeded as outlined in the previous sections. RE silicide additions occurred during tapping. The RE silicide was also introduced during tap. The method of addition varied based on the experimental condition. Typical practice in previous experiments had been to add the RE silicide into the tap stream while filling the ladle. This was done to serve as a baseline for comparison with the other techniques. The author had postulated that improving RE element recovery would improve refinement. One approach placed 0.3 wt. % RE silicide into a small plain carbon steel tube that was welded closed on one end. Then, the tube was placed on the bottom of the ladle prior to tapping. The author also attempted to create higher sulfur content RE oxysulfides by placing a mixture of RE silicide and iron pyrite into a closed one end steel tube that was placed on the ladle bottom prior to tapping. In another method, a 0.3 wt. % RE silicide addition was coated with zinc and then introduced into the stream during tapping. The final method was the addition of 0.3 wt. % RE silicide by an aluminum coated RE silicide addition. After tapping, the heat cooled to 1620°C prior to pouring.

The yield strength (YS) and ultimate tensile strength (UTS) of each heat are plotted in Figure 6. The yield strength and UTS of the baseline steel with no RE additions were 276 MPa and 527 MPa respectively. Heats with the highest cerium content did have the highest average YS; however, only the 0.3 RE bars had a yield strength and UTS statistically higher than the baseline heat. Optical microscopy found that all of the treated steels had a finer structure, which did not correlate to the observed mechanical properties. SEM analysis with EDS of the inclusions found that the inclusions formed in only the 0.3 RE steel and 0.3 RE tube steel had the typical RE oxy-sulfide inclusions observed in previous experiments by the PI. The RE tube treated steels however had fewer RE inclusions than the 0.3 RE addition steel. The other steel treatments produced very different inclusions that did not appear capable of refining the structure through a heterogeneous nucleation mechanism. These other addition methods tended to produce high inclusion contents which likely decreased the steel's strength. This would explain why the steels were finer than the baseline, but had the same strength.

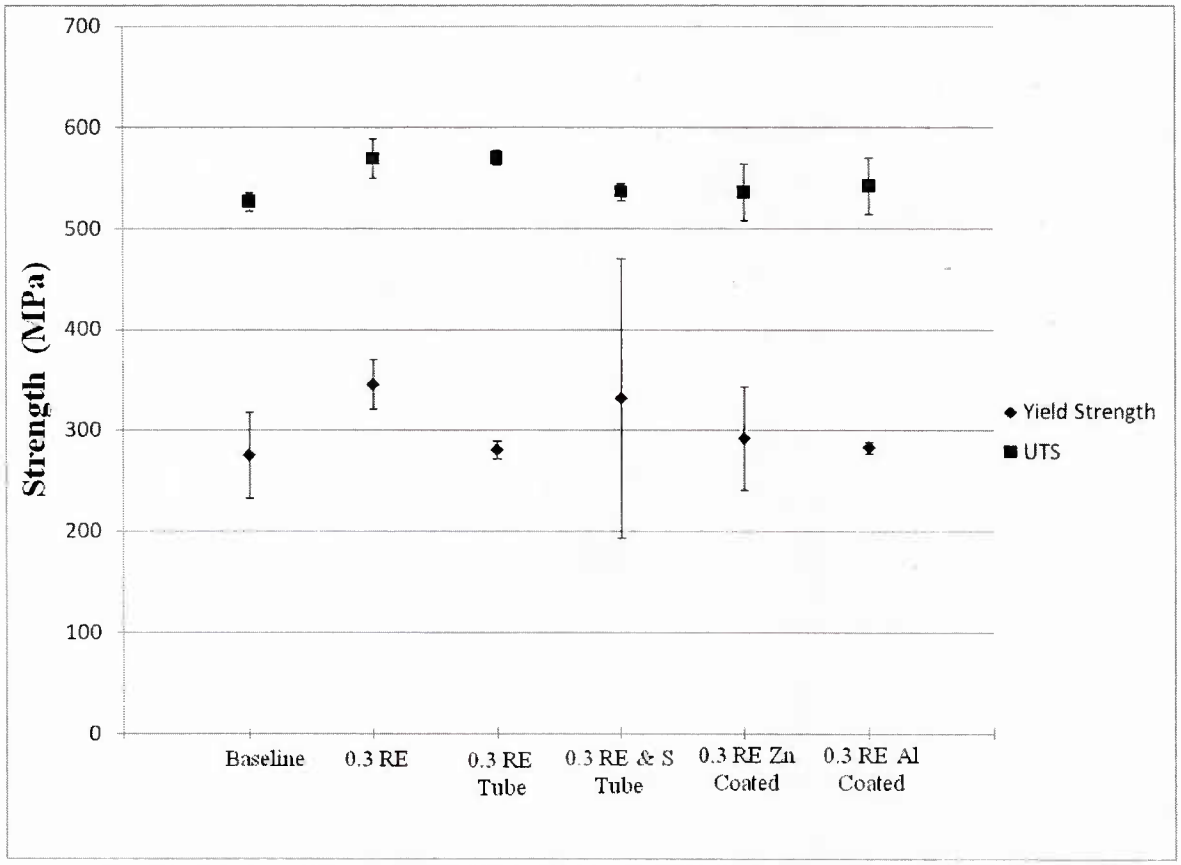

Figure 24 Yield strength and ultimate tensile strength as a function of the addition method.

Early work by the PI attempted to use titanium additions for grain refining steels. These early attempts found that the addition of titanium refined the microstructure, but had done so through grain boundary pinning and not acting as heterogeneous nuclei. This was because CALPHAD calculations predicted that the titanium carbonitrides observed in the microstructure formed very late in solidification and would not have been active heterogeneous nuclei. However, TiC has been theorized to act as a nuclei due to its very close crystallographic match with δ-ferrite, the primary phase in carbon steels. Based on this theory, the PI thought that despite the thermodynamic instability of TiC in molten steel that a large TiC particle

might survive long enough to decrease in size and act as a heterogeneous nuclei. To do this the TiC particles would have to be very large. Such large particles would not be feasible to form in a steel melt. However, a high carbon melt might provide the necessary carbon content. Using Thermo-Calc©, the author determined that it was possible to form TiC in a ferrous melt (2 wt. % C, 2 wt. % Si, 4.3 wt. % Ti) as the primary phase.

To create the TiC master alloy, cast iron scrap, steel scrap, and FeSi were melted in an induction furnace. Once all the initial charge was melted, the melt was brought to 1480°C before adding the FeTi. The FeTi had to be stirred in due to the immediate formation of TiC in the melt. As predicted by Figure 9, the melt immediately became very slushy due to the large (~15%) solid fraction that formed. This was poured into a mold consisting of six 1 in. diameter, by 3 in. tall cylinders. After pouring, the test castings were sectioned into smaller sizes for creating plate test castings from 1030 steel. Also a sample was prepared for metallographic examination in the optical and scanning electron microscopes.

Figure 25 depicts the microstructure of the TiC master alloy formed. The presence of a significant level of titanium carbides is evident. SEM analysis determined that the dark phases in Figure 10 are titanium carbides.

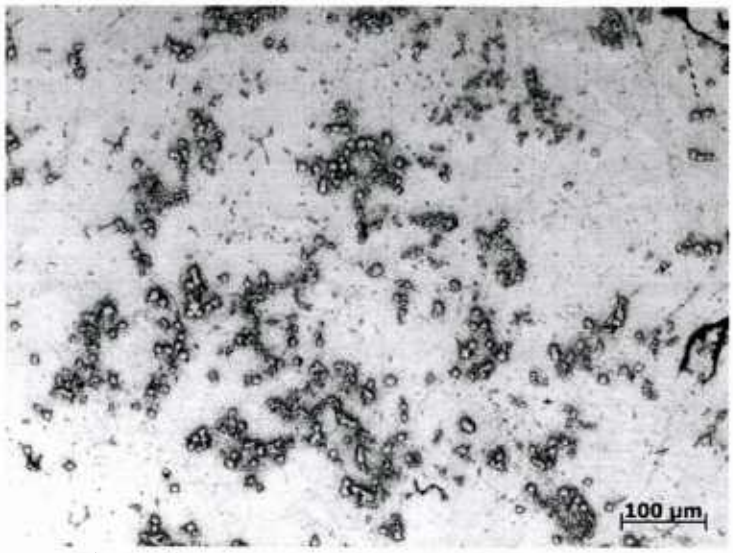

Figure 25 Optical micrograph of the TiC master alloy.

Plate castings using the same pattern and melting procedure outlined in the previous section were used. Upon tapping at 1720°C, aluminum shot and the TiC master alloy additions occurred. Target compositions of 0, 0.1 wt. %, and 0.3 wt.% Ti were done. The castings cooled for several hours to ensure the same cooling rate through the eutectoid reaction. Samples for tensile bars, metallurgical specimens, and spectroscopy were extracted.

Figure 26 depicts the strength levels attained with this master alloy. Yield strengths between the heats were statistically similar. Significant variation in yield strength occurred in the TiC master alloy treated heats. The TiC master alloy heats had statistically higher UTSs than the baseline, but were not different from each other. Microscopy found no significant differences between the treated steels and the baseline material, consistent with the mechanical property data. SEM examination of the TiC master alloy treated samples found no evidence of titanium carbides or carbonitrides in them. It appears that the TiC particles dissolved in the melt in accordance with the predicted phase equilibrium.

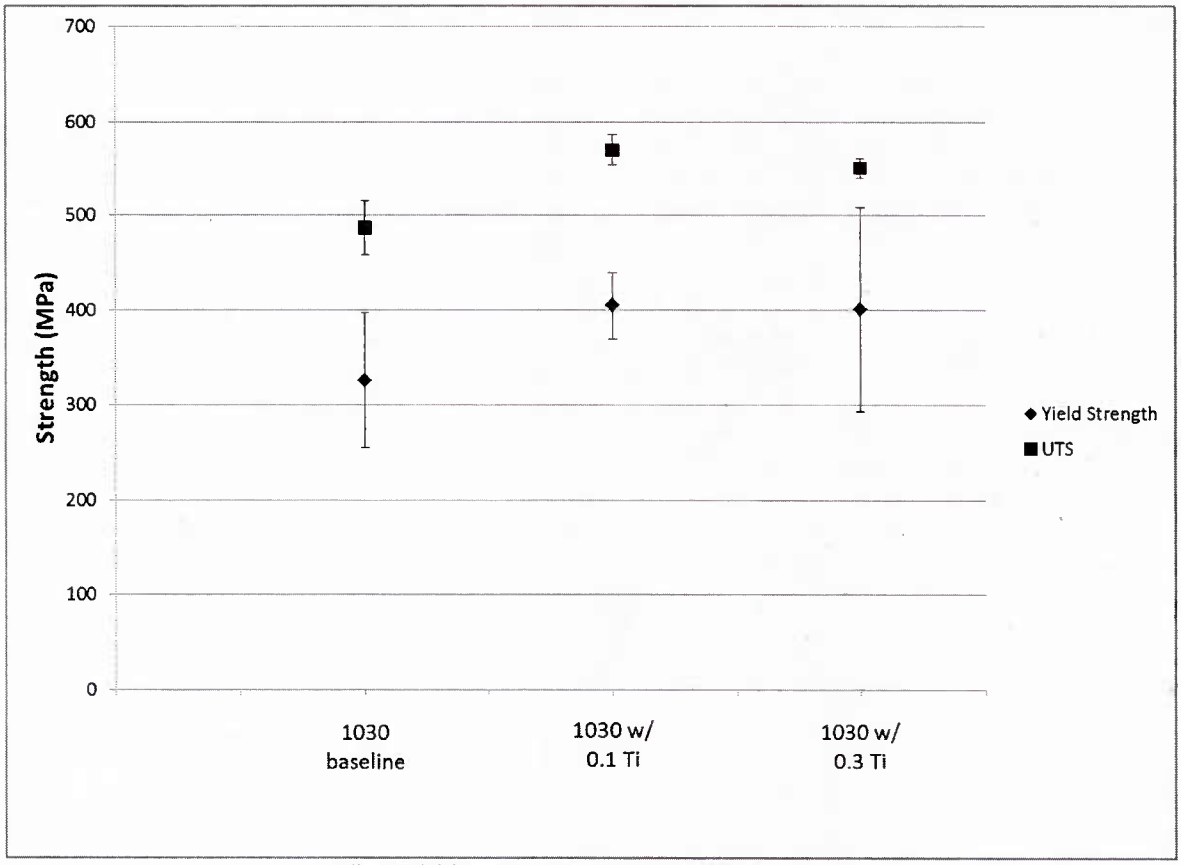

Figure 26 Strength verses TiC Master addition.

RE based master alloys were created and experimented with so that the inclusion composition could be more easily controlled than ladle additions allow. The goal of these experiments had been to assist with determining which types of inclusions play the primary role in acting as heterogeneous nuclei. RE oxides and oxysulfides have been detected in earlier work by the PI.[4,5, 8,9] It is still not apparent which inclusions play the primary role.

Master alloy manufacturing occurred in a small 1600°C resistance furnace. Iron granules, RE silicide, iron pyrite, and ferroaluminum were placed into 10 mL high alumina crucibles with alumina covers. The exact composition of the charge varied depending on if RE oxides, RE oxysulfides, or RE aluminum oxides were being formed. Each sample had a total mass of 54 g. Three crucibles would be placed inside a larger alumina crucible. Graphite encased the smaller alumina crucibles to ensure only the oxygen within the crucible was available for the reactions. An alumina plate covered the larger crucible, which was then placed in the furnace. The furnace heated the samples at a rate of 10°C per minute until 1570°C was achieved. They then were held for half an hour before cooling at a rate of 10°C per minute.

A series of RE oxide (RE-O), RE sulfide (RE-S), and RE aluminum oxide (RE-O Al) inclusions were formed in the master alloys. The RE-O and RE-S master alloys had good homogeneity when removed from the 10 mL crucibles; however, the RE-O Al master alloys showed evidence of insufficient melting and heavy oxide coatings around the RE silicide particles. The target temperature was reached since the

iron granules melted so it appears the oxide coating around the RE silicide particles prevented their fusion with the rest of the melt.

SEM/EDS analysis of the particles found that a variation in oxide and sulfide composition was achieved. In the RE-O master alloy, the particles consisted of a very RE rich oxide particle with iron and a little silicon. This is similar to the RE oxides found by the author in other work. The RE-S master alloy had RE sulfides with significant levels of iron in them. They also had a complex appearance. These had higher sulfur levels than the RE oxysulfides or sulfides observed by the other. However despite containing multiple RE elements, these RE sulfides were similar to CeS type inclusions Unlike the RE-O and RE-S master alloys, the Re-O Al master alloy had poor homogeneity and RE aluminum oxides were only observed on the surface of RE silicide pieces. While SEM analysis found some RE aluminum oxides, their composition did not match the composition typically observed in the PI's previous work (See Table 10). The aluminum levels in the inclusions were on the 1-5 wt.% not the 20 wt. % level. It appeared that the ferroaluminum tended to oxidize at a significantly lower temperature than the RE silicide. All of the RE-O Al master alloy samples had aluminum oxide on top of them when removed from the furnace. This and the low aluminum level of the RE aluminum oxides indicates that most of the aluminum oxidized prior to melting of the charge. Efforts to prevent this did not meet success. The samples were still used in the event that they contained effective nuclei. Plate castings were then produced using each master alloy. As an additional control, a heat was poured with a 0.3 RE silicide addition conducted in the same manner as the PI's previous experiments.

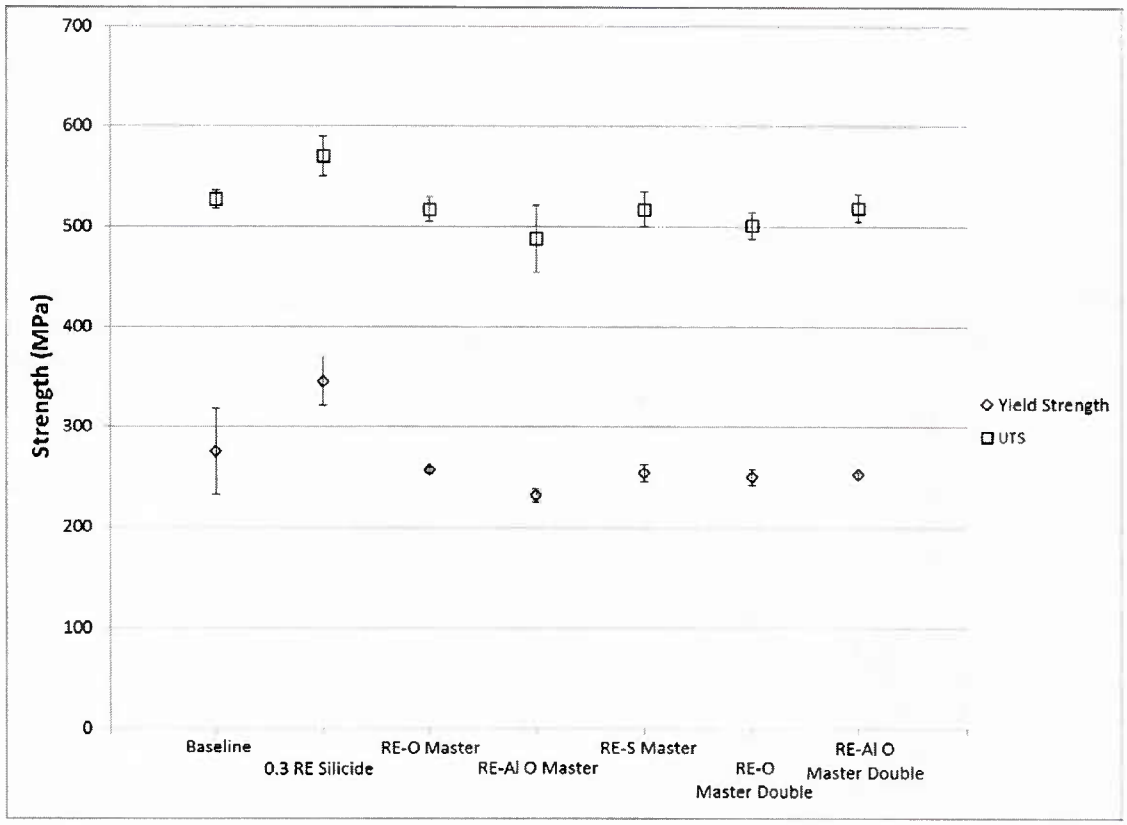

Figure 27 Yield strength and UTS as a function of the master alloy addition.

The yield strength and ultimate tensile strength (UTS) for each heat is depicted in Figure 27. The error bars represent a 95% confidence interval. All three of the RE master alloy heats had yield strengths statistically similar to the baseline heats average of 276 MPa. Their UTSs, at approximately 500 MPa, were slightly lower than the baseline (526 MPa), but still statistically similar. The 0.3 RE silicide heat had a higher yield strength (346 MPa) and UTS (570 MPa) than the baseline material. SEM analysis found that the RE master alloy addition heats either had no or very few RE inclusions. It appears that agglomeration of the inclusions during addition occurred which prevented the inclusions from being effective nuclei.

Task 8: Grain Refined Steel Rolling Experiments

Most of the effort by the PI has been on examining the creation of a grain refinement method for foundries. However, the wrought steelmaking industry should be able to benefit from the use of a solidification based grain refiner. Due to the fact that the technology requires the creation of inclusions, the PI had some reservations regarding their impact on the rolling performance of the steel. To address this and document how mechanical properties evolved ruing rolling, the PI conducted a set of rolling experiments. Three plates with either no addition or 0.3 % RE silicide were poured using the same melting and casting procedures outline earlier in this report. Portions of each casting were extracted to make a 100 mm by 142 mm by 22mm plate for rolling, an as-cast metallographic sample, and a spectrometer sample. These plates were then rolled in a 355 mm Fenn rolling mill at 10 rpm. Target reductions of 10%, 25%, and 50% were done. After rolling, subsized flat tensile bar samples were extracted and tested in accordance to ASTM E8.

No cracking occurred in any of the plates. Figures 28 and 29 show the initial and final states of the plates. No significant differences between the baseline and treated plates were noted during processing. The level of plate distortion due to rolling did not appear to be significantly different between the materials. Hardness measurements found that the treated steels tended to have a higher hardness before and after rolling than the baseline material. The lack of difference between the baseline and 0.3 RE silicide treated steels indicates that the RE oxide and oxysulfides inclusions do not appear to have a detrimental impact on the rolling performance of this steel grade.

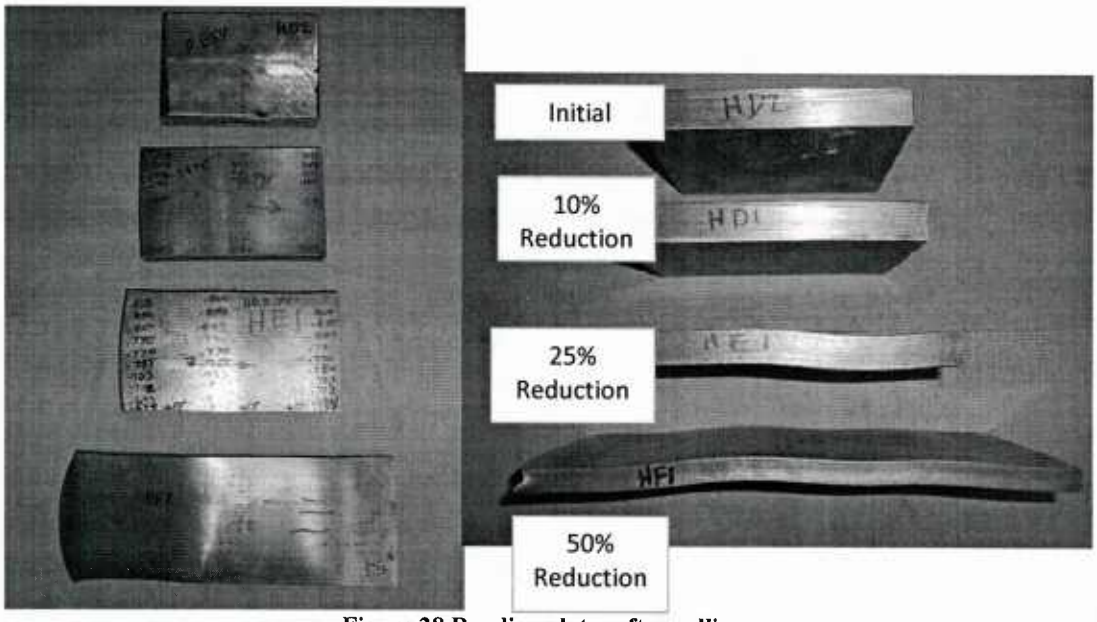

Figure 28 Baseline plates after rolling.

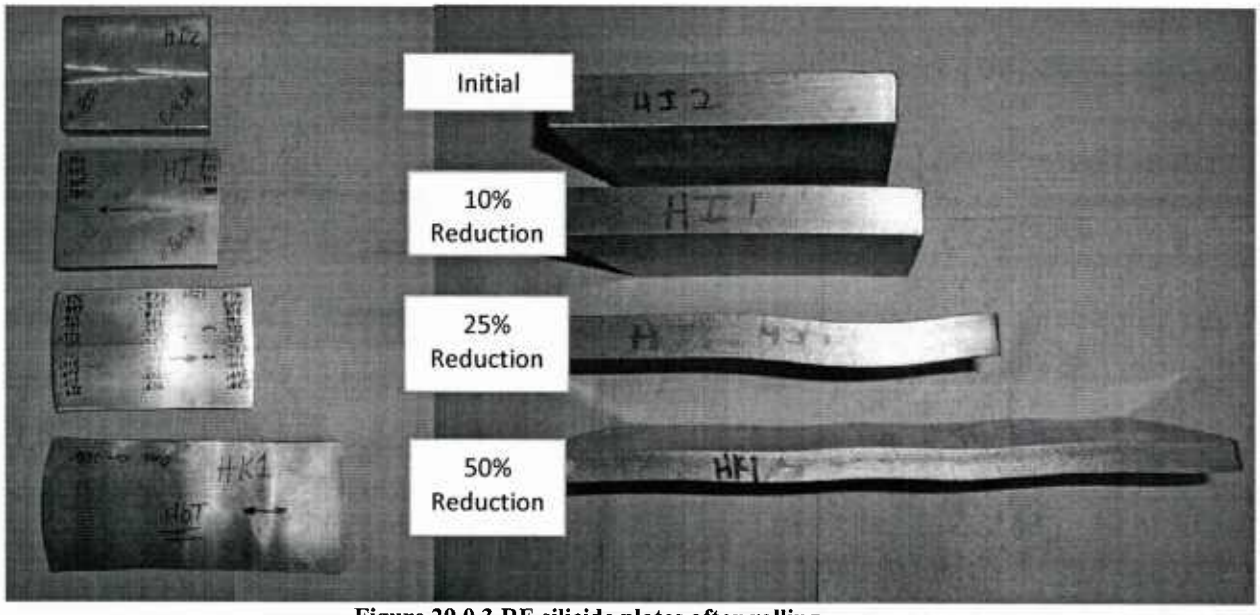

Figure 29 0.3 RE silicide plates after rolling.

As expected the yield strength and ultimate tensile strength (UTS) increased with the amount of cold work (See Figures 30 and 31). The 0.3 RE silicide treated steels had statistically higher strengths at 10% and 25% cold work; however, no difference in behavior was observed once 50% cold work was achieved. The increase in yield strength and UTS was approximately 15% for the lower cold work specimens.

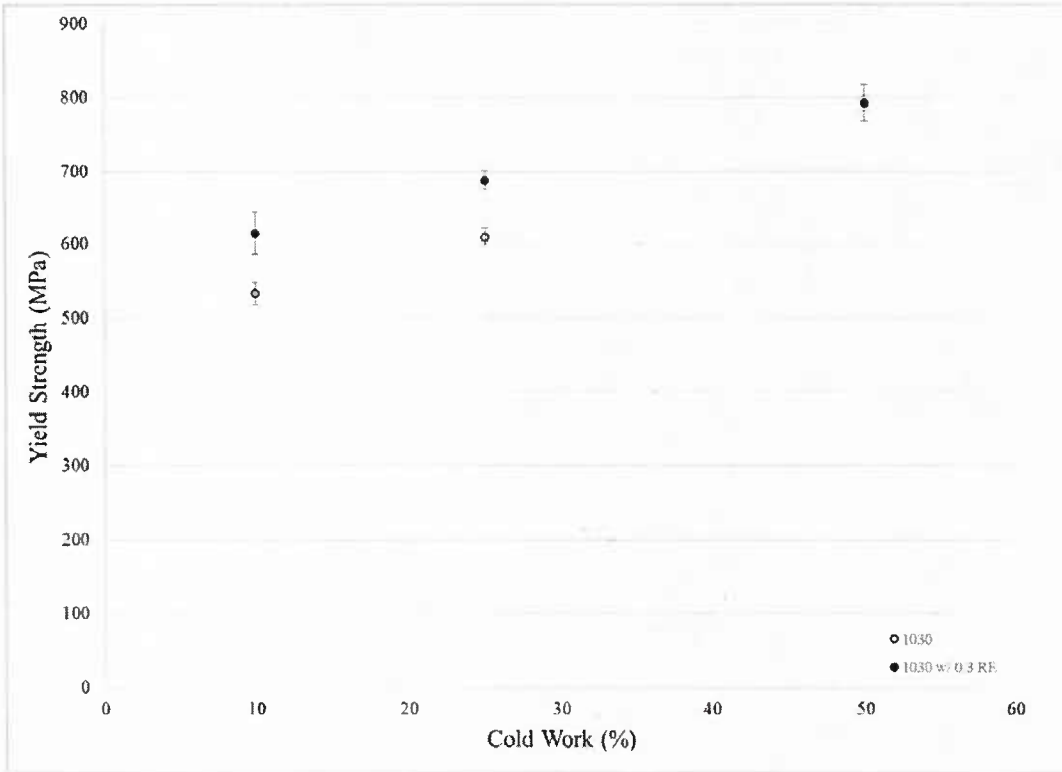

Figure 30 Effect of cold work on yields strength.

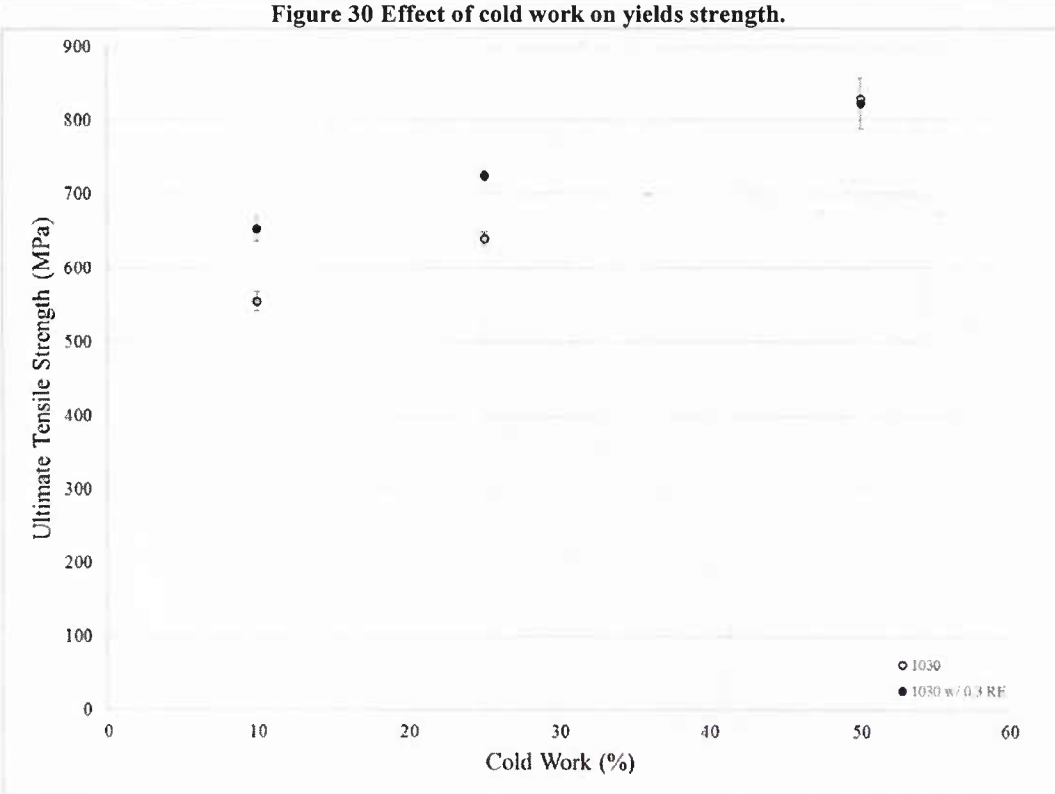

Figure 31 Effect of cold work on ultimate tensile strength.

Task 9: Additional RE Based Master Alloys

Towards the end of the original project, the PI had developed a new concept on how to create master alloys. This was primarily driven by the realization that the previously attempted RE Master Alloys may have suffered from a lack oxide formation. Thus as part of the project's no cost extension, the PI included a new set of master alloy experiments. To create the master alloys, the author melted a heat of 1001 HP stock in the furnace. No alloy additions were made to ensure sufficient oxygen was available in the melt to create RE oxides. A small amount of the heat was tapped into a hand ladle to create five pound amounts of the target master alloy. In each hand ladle varying amounts of RE silicide, EGR, iron pyrite, and aluminum were added. The most promising master alloys were a RE master, a RE-Al master, and an EGR master. The other alloys created, particularly the RE-S masters, did not contain the appropriate RE based inclusions for refinement. These master alloys were then poured into plate castings using the procedure outlined previously. Tensile bars were then sectioned from these to

Figure 32 depicts the strength for each master alloy addition. None of the master alloys had a strength higher than the baseline no addition steel. Optical microscopy found no difference in average free ferrite grain size. SEM analysis found that all of the additions tended to form a RE silicate type inclusion instead of the desired RE oxy-sulfide. These RE silicate inclusions were rounded which indicates that they were liquid at steelmaking temperatures. The PI postulates that the lack of refinement was due to these inclusions being a liquid and not solid during casting.

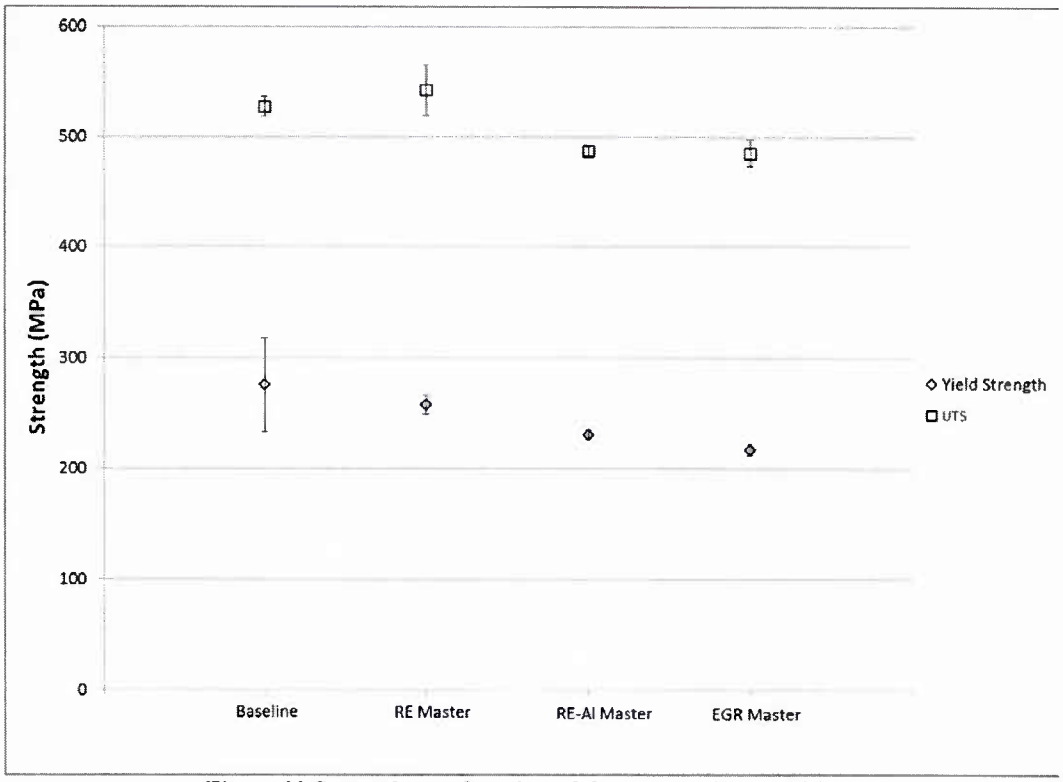

Figure 32 Strength as a function of the master alloy addition.

The project has successfully met all of the tasks originally proposed as well as those added under the no cost extension. While the PI is still publishing out the results from this project, they have certainly added to our understanding of the grain refinement of steels.